Received: 8 September 2021 | Accepted: 9 September 2021 | Published on: 6 October 2021

DOI: 10.1002/net.22078

SPECIAL ISSUE ARTICLE

WILEY

Autonomous traffic at intersections: An optimization-based analysis of possible time, energy, and CO_2 savings

Do Duc Le[1] | **Maximilian Merkert**[1] | **Stephan Sorgatz**[2] | **Mirko Hahn**[1] | **Sebastian Sager**[1]

[1]Faculty of Mathematics, Otto-von-Guericke University Magdeburg, Magdeburg, Germany
[2]Volkswagen Aktiengesellschaft, Wolfsburg, Germany

Correspondence
Maximilian Merkert, Technische Universität Braunschweig, Universitätsplatz 2, 38106 Braunschweig, Germany.
Email: m.merkert@tu-braunschweig.de

Present address
Maximilian Merkert, Technische Universität Braunschweig, Universitätsplatz 2, 38106 Braunschweig, Germany

Funding information
Deutsche Forschungsgemeinschaft; Volkswagen Group Research and Group Strategy.

Abstract

In the field of autonomous driving, traffic-light-controlled intersections are of special interest. We analyze how much an optimized coordination of vehicles and infrastructure can contribute to efficient transit through these bottlenecks, depending on traffic density and certain regulations of traffic lights. To this end, we develop a mixed-integer linear programming model to describe the interaction between traffic lights and discretized traffic flow. It is based on a microscopic traffic model with centrally controlled autonomous vehicles. We aim to determine a globally optimal traffic flow for given scenarios on a simple, but extensible, urban road network. The resulting models are very challenging to solve, in particular when involving additional realistic traffic-light regulations such as minimum red and green times. While solving times exceed real-time requirements, our model allows an estimation of the maximum performance gains due to improved communication and serves as a benchmark for heuristic and decentralized approaches.

KEYWORDS

autonomous driving, cooperative systems, energy-efficient mobility, extended formulations, microscopic traffic modeling, mixed-integer programming, moving-horizon methods, traffic optimization

1 | INTRODUCTION

Assisted and autonomous driving is a growing field of interest and has been gaining importance in research and public awareness. Many car manufacturers, research institutes, and related industries have been researching along these lines, cf. [10, 27, 33, 34, 40], and been making efforts to develop and evaluate the impact of systems in such contexts. Autonomous driving, which is the ultimate consequence of assisted driving and can—according to the *German Association of Automotive Industry (VDA)*—be classified into five levels, considers the movement of the individual car in the first place. Simply put, an autonomously driving car is mainly concerned with moving to its destination in an accident-free and regulation-compliant manner. Qualifying quantities such as *traffic flow* are of minor interest and therefore barely or not at all considered in current implementations. Le Vine et al. [21] suggest that traffic flow could even get worse when autonomously driving cars are introduced.

On the other hand, there are cooperative systems. They are in general independent from assisted or even autonomous driving and aim to generate benefit for the involved cars, or infrastructural devices, by exchanging information. A very simple example for a cooperative system following this definition are turn signals. The growing field of technology and

devices for wireless communication promises to facilitate the process of exchanging information between traffic participants. Among other technologies, wireless LAN, which in the automotive context is often referred to as *vehicle-to-vehicle* (*V2V*) and *vehicle-to-X* (*V2X*), is of current interest. It offers sufficiently wide ranges, short delays, and direct communication between agents, cf. [2]. With the technological advances in autonomous mobility, the coordination of vehicular traffic offers new possibilities for increasing traffic efficiency—especially at urban intersections which represent intrinsic bottlenecks for the movement of cars. Our goal is to quantify this anticipated potential to reduce waiting time, energy consumption, and CO_2-emissions and to analyze a variety of scenarios, including different traffic densities and traffic-light regulations.

1.1 | Related work

There are a huge number of contributions on the coordination of connected and automated vehicles at intersections, see [4, 13, 18, 24, 32] for survey papers. Most contributions propose heuristic rules to determine the order in which vehicles may cross the intersection. For example, the works of Dresner and Stone [5] propose a reservation scheme with a central control unit. Vehicles are treated as driver agents and send requests of timeslots to cross the intersection which are then either accepted or rejected by the central control unit based on certain rules. Ahn and Del Vecchio [1] propose a supervisory algorithm for intersections with multiple lanes from each direction and many conflict zones, but only consider a single vehicle per lane. They model the safety verification problem as a job-shop scheduling problem, which is then approximated via mixed-integer linear programming (MILP) models. In [14, 15], Hult et al. [26, 42] propose a decentralized optimal control framework which minimizes energy consumption subject to maximizing the throughput using a first-in-first-out heuristic to decide on the order in which the vehicles cross the intersection. The authors in [12] construct a discrete-time discrete-space model which can be divided into cells and provide graph-based algorithms to minimize the total completion time. A number of references using approaches based on optimization and optimal control can be found in [32]. For example, in [22], the authors formulate a nonlinear constraint optimization problem, which tries to find optimal vehicle trajectories by minimizing the overlap of vehicle positions inside the intersection area. The solution is then used by a controller to construct passing sequences. Still, the models are often too complex to calculate a global system optimum, and hence fall back to approximation heuristics. Considerable reductions not only in travel time and delays, but also in fuel consumption are possible for centrally controlled traffic at intersections or highway on-ramps (see e.g., [32, tab. I]). Still, the reported methods were mostly heuristic-based and the overview table from this survey lists no publications from the category "Optimization and Control" that explicitly provide such figures. Developing policies that use few computational resources and can directly be realized with current technology has been the predominant motivation so far. However, the derivation of bounds on what could possibly be achieved with optimum communication has been widely neglected in comparison and only few works aim for provable global optimality. An example is [41]. The authors consider intersection control for platoons of automated and conventional cars approaching an intersection. Their approach is not MILP-based, but uses a branch-and-bound algorithm with custom bounding techniques in order to cut the number of possible passing sequences that have to be considered.

Our work provides some analysis on which improvements one can expect from the viewpoint of global optimality that can then serve as a comparison tool for other approaches such as heuristic-based methods. Furthermore, while most of the recent work omits traffic-light regulations and focuses on the collision-free traversal of the vehicles, we include these into our considerations. Due to a considerable amount of technology for the exchange of information and other purposes, traffic-light controlled intersections provide an extendable infrastructure and are therefore a reasonable setting for exemplary study. Only few studies address the simultaneous optimization of traffic-light signals and vehicle operations (see e.g., [13, tab. II]). One such method mentioned in this survey is, for example, [25]. In order to solve the problem, they enumerate feasible signal timing plans and determine for each the optimal vehicle trajectories. But this is done on a simple network with two single-lanes and no turning movements. Additionally, while some studies report numbers on possible reductions in travel time or fuel consumption, the explicit effect of traffic lights on those is far from explored. Our model can describe different traffic-light scenarios, thus giving insight into the influence of certain traffic-light regulations on the resulting traffic.

1.2 | Goals and organization of the paper

We study traffic at traffic-light controlled intersections by regarding each car individually, and by centrally optimizing traffic flow to global optimality. To this end, we develop a MILP with variables for states of both the cars and the traffic lights on a fixed time horizon. The model has been introduced in the dissertation of Sorgatz [35], on which this work in part is based. We extended it in several aspects, for example, by incorporating right and left turns. In contrast to other publications, our model allows for an easy consideration of different traffic-light regulations and we obtain globally optimal solutions for a centrally coordinated

traffic flow. While the resulting MILPs turn out to be too hard to solve for real-time requirements, the offline-calculated solutions can serve as a benchmark for evaluating other approaches, for example, heuristic solution methods, for improving traffic flow at intersections. Also model-predictive control algorithms [31] in general and for mixed-logic systems in particular [9] can be benchmarked against these bounds, as we shall already do here. Last but not least, the global results can be used for a sensitivity analysis to evaluate the impact of different influencing factors (such as traffic-light legislation) on the potential for improving traffic efficiency. Due to the focus of this paper in providing valid bounds, our model idealizes several aspects, which includes assuming no communication delays and perfect information—thus leaving aside for example, low-level spacing and gap control.

The paper is organized as follows. We describe the model in Section 2. In Section 3 we specify the numerical experiments. We give numerical results and compare different scenarios in terms of runtime and the achieved objective value in Section 4. Additionally, the resulting traffic flow is evaluated with respect to the performance indicators time, energy, and emissions with the aid of microscopic traffic simulations. Concluding remarks are given in Section 5.

2 | SIMPLE MOVEMENT MODEL AND GLOBAL-MILP

In this section, we develop a MILP which describes the traffic flow of all cars on a simple urban road network on a fixed time interval $\mathcal{T} := [0, t_f]$. In addition to the behavior of all cars at any time step, we also optimize the signal states of the traffic lights in the network.

The basic structure of our scenario is as follows: two straight roads intersect in a single intersection. Each road consists of two lanes running in opposite directions. In each lane, a traffic light *tl* from the set of traffic lights *TL* regulates traffic flow from that lane into the intersection. For simplicity, we keep to this simple example to introduce the model. Note, however, that the model can be straightforwardly extended to represent networks with multiple intersections, more than two intersecting roads and multiple lanes.

As we want to determine the optimal movement of the cars along the road offline, only the time each car enters the network, called *arrival time* $t_{\text{init},c} \in \mathcal{T}$, and its velocity $v_{\text{init},c} > 0$ at this time are fixed. All cars enter the network on a particular lane at the same position, which is simply labeled 0.

To obtain a microscopic traffic model, we need model components for

- the longitudinal movement of each car,
- the logic of traffic lights,
- traffic-light regulations, such as minimum lengths of red and green phases,
- collision prevention on intersections,
- collision prevention on lanes, before and after possible turning maneuvers,
- a meaningful objective function.

In the following, we will discuss them one by one.

2.1 | Car motion model

For the purposes of the model, a car c in the set of all cars C is a moving occupant of a stretch of road. At any given time, it moves on a road using a specific lane. A lane may be used by multiple cars. Two cars using the same lane may not simultaneously occupy the same space within that lane. We refer to our efforts to prevent this as *collision prevention*. Note that we only consider longitudinal movement, which means that overtaking maneuvers are forbidden.

The movement of any given car is governed by the following laws of motion. As friction is negligible in an urban setting, we focus on linear constraints which means a trade-off between realism and low runtimes.

$$
\begin{aligned}
\dot{s}(t) &= v(t) && \forall t \in \mathcal{T},\\
\dot{v}(t) &= a(t) && \forall t \in \mathcal{T},\\
\dot{a}(t) &= j(t) && \forall t \in \mathcal{T},\\
s(t_{\text{init},c}) &= 0,\\
v(t_{\text{init},c}) &= v_{\text{init},c},\\
v(t) &\in \left[\underline{v}, \overline{v}\right] && \forall t \in \mathcal{T},\\
a(t) &\in \left[\underline{a}, \overline{a}\right] && \forall t \in \mathcal{T},\\
j(t) &\in \left[\underline{j}, \overline{j}\right] && \forall t \in \mathcal{T}.
\end{aligned}
\tag{1}
$$

In the ODE-system (1), $s(t)$ is the traveled distance of the car, measured by the position of the car's front on the lane at time t. Its velocity is encoded in $v(t)$, $a(t)$ is its acceleration, and $j(t)$ its jerk. The bounds $0 \leq \underline{v} < \overline{v}$, $\underline{a} < 0 < \overline{a}$, and $\underline{j} < 0 < \overline{j}$ are due to physical and comfort restrictions and set for each car individually. The linear ODE-system is discretized using an equidistant discretization of $\mathcal{T}$. Let $T := \{0, \dots, N\}$ and $T_c := \{t_{\text{init},c}, \dots, N\}$. The explicit Euler method on T and T_c with step length $dt := T/N$ is an appropriate choice for the rather simple motion model. This yields the following system of equations:

$$s_{c,t+1} = s_{c,t} + v_{c,t} \cdot dt \qquad \forall c \in C,\ t \in T_c \backslash \{N\}, \tag{2}$$

$$v_{c,t+1} = v_{c,t} + a_{c,t} \cdot dt \qquad \forall c \in C,\ t \in T_c \backslash \{N\}, \tag{3}$$

$$s_{t_{\text{init},c}} = 0 \qquad \forall c \in C, \tag{4}$$

$$v_{t_{\text{init},c}} = v_{\text{init},c} \qquad \forall c \in C, \tag{5}$$

$$\underline{v}_c \leq v_{c,t} \qquad \forall c \in C,\ t \in T_c, \tag{6}$$

$$v_{c,t} \leq \overline{v}_c \qquad \forall c \in C,\ t \in T_c, \tag{7}$$

$$\underline{a}_c \leq a_{c,t} \qquad \forall c \in C,\ t \in T_c, \tag{8}$$

$$a_{c,t} \leq \overline{a}_c \qquad \forall c \in C,\ t \in T_c, \tag{9}$$

as well as the inequalities:

$$\underline{j}_c \leq \frac{1}{dt} \cdot \left(a_{c,t+1} - a_{c,t}\right) \leq \overline{j}_c \quad \forall c \in C,\ t \in T_c \backslash \{N\}. \tag{10}$$

For simplicity, we demand $t_{\text{init},c} \in T$.

2.2 | Traffic lights

As our main goal is to model traffic at urban intersections, traffic lights play a very important role since they manage collision prevention between cars driving on different lanes.

In principle, traffic lights are designed for human drivers and not strictly required in fully autonomous traffic, as is for example, remarked in [5]. However, while our model assumes centrally controlled vehicles, we want to allow benchmarking of methods designed for mixed-traffic scenarios, that is, with autonomous and human drivers. See [3] for first studies in this direction. Furthermore, we are able to distinguish performance gains due to increased communication from gains that are due to relaxing traffic-light regulations, which may be imposed by law. Please note that while physical traffic lights are superfluous for autonomous cars, right of ways still has to be modeled for intersections. Our model presented in the following would be the same if there were no physical traffic lights, except for the constraints implementing minimum red and green phases in Section 2.2.2.

In this section, we introduce traffic light triggers to model the regulatory effect of traffic lights. A basic insight is that an interaction between traffic lights and cars always yields constraints that are only relevant for cars that enter specific sections of the road. For instance, an intersection between two lanes is essentially a small section on either lane that cannot be driven on freely. We will refer to such a section as an *intersection area.*

2.2.1 | Right of way

For each traffic light tl of the of the intersection and for each time step $t \in T$, we introduce a state variable $\chi_{tl,t}$. We can interpret a traffic light tl having a green light at time step t if the corresponding variable $\chi_{tl,t}$ equals 1. If $\chi_{tl,t} = 0$ holds, the traffic light is set to red. We now consider a single intersection with its set of traffic lights TL, where usually $|TL| = 4$. For this set, we define a decomposition into subsets

$$TL = \bigcup_{k=1}^{K} TL_k,$$

where $K \in \mathbb{N}$ and the sets TL_k contain *conflicting* traffic lights. Conflicting means that only a single traffic light $tl \in TL_k$ is allowed to be set to green in each time step. This is enforced by the constraint:

$$\sum_{tl \in TL_k} \chi_{tl,t} \leq 1 \qquad \forall t \in T,\ k \in \{1, \dots, K\}. \tag{11}$$

In particular, if the network consists of a single intersection and all traffic lights are conflicting, it holds that $K = 1$. Theoretically, it is also possible to declare traffic lights belonging to different intersections as conflicting.

2.2.2 | Limiting the green and red phase

For some of our later considerations, we want to impose limits on the duration of the *green* and *red phase*. These are the time frames during which cars may or may not enter the intersection. To avoid traffic lights switching rapidly between red and green, we demand that the traffic light has to stay green for some period of time after switching from red to green and similarly has to stay red for a given minimum amount of time before it can switch to green again. The same problem appears in the unit commitment context where electrical generators for energy production are coordinated [37]. The generators need to stay active (inactive) for some duration when turned on (off). This problem is often referred to as *minimum up/down time* in the literature. We use an extended formulation which originated from Rajan and Takriti [30], based on a complete linear description of the so-called min-up/min-down polytope by Lee et al. [23].

The description of the problem is given by the following *turn on/off inequalities*:

$$\chi_{tl,t} = \chi_{tl,t-1} + \overline{y}_{tl,t} - \underline{y}_{tl,t} \qquad \forall tl \in TL,\ t \in \{1, \dots, N\}, \tag{12}$$

$$\sum_{i=t-L+1}^{t} \overline{y}_{tl,i} \leq \chi_{tl,t} \qquad \forall tl \in TL,\ t \in \{L, \dots, N\}, \tag{13}$$

$$\sum_{i=t-l+1}^{t} \underline{y}_{tl,i} \leq 1 - \chi_{tl,t} \qquad \forall tl \in TL,\ t \in \{l, \dots, N\}. \tag{14}$$

As stated before, the binary variable $\chi_{tl,t}$ describes the state of the traffic light tl at time step t and is 1 for green and 0 for red. Newly added binary variables $\overline{y}_{tl,t}$ and $\underline{y}_{tl,t}$ model the switching from red to green and green to red, respectively. The second inequality implies that there will be at most one switch from red to green in the last L time steps if $\chi_{tl,t} = 1$ and zero switches from red to green if $\chi_{tl,t} = 0$. This guarantees a green phase of length at least L. Similarly, the third inequality gives us a red phase of length at least l. Note that (12)–(14) represent a significant improvement over the formulation in [35] with respect to computational efficiency.

2.2.3 | Traffic light triggers

In order to enable and disable constraints based on the location of the car, we use big-M formulations. Therefore, let $\underline{s}$ and $\overline{s}$ be lower and upper bounds for the distance variables $s_{c,t}$ of car c. Furthermore, we consider a traffic light trigger with associated intersection area $\left[s^{\text{start}}, s^{\text{end}}\right]$ with $\underline{s} \leq s^{\text{start}} < s^{\text{end}} \leq \overline{s}$. As we only regard a single car for our considerations in this subsection, we omit the indices for its individual variables. We do the same for indices of a single traffic light and the time interval.

We use an "enter-leave formulation," where we introduce two binary indicator variables χ_t^{in} and χ_t^{out} for each combination of car and traffic light. We want to ensure the relations

$$\left(\chi_t^{\text{in}} = 0\right) \Rightarrow \left(s_t \leq s^{\text{start}}\right) \quad \text{(car has not entered intersection area)}, \tag{15}$$

$$\left(\chi_t^{\text{out}} = 0\right) \Rightarrow \left(s_t \geq s^{\text{end}}\right) \quad \text{(car has already left intersection area)}. \tag{16}$$

They can be implemented by the big-M constraints

$$\left(s^{\text{start}} - \overline{s}\right) \cdot \chi_t^{\text{in}} + s_t \leq s^{\text{start}} \qquad \forall t \in T, \tag{17}$$

$$\left(s^{\text{end}} - \underline{s}\right) \cdot \chi_t^{\text{out}} + s_t \geq s^{\text{end}} \qquad \forall t \in T, \tag{18}$$

where $(s^{\text{start}} - \overline{s})$ and $(s^{\text{end}} - \underline{s})$ represent feasible values for big-M, respectively, such that no restriction is imposed if the enter-leave variables are set to 1.

It follows that

$$s_t \in \left(s^{\text{start}}, s^{\text{end}}\right) \Rightarrow \left(\chi_t^{\text{in}} = 1 \wedge \chi_t^{\text{out}} = 1\right),$$

that is, both χ_t^{in} and χ_t^{out} are equal to 1 if the car is inside the intersection area (but not necessarily vice versa). This case is only allowed if the traffic light for the corresponding lane and intersection shows green, which can be guaranteed by the constraint

$$\chi_t^{\text{in}} + \chi_t^{\text{out}} - \chi_t \leq 1 \quad \forall t \in T. \tag{19}$$

When $s_t \notin \left(s^{\text{start}}, s^{\text{end}}\right)$, it is ensured that either χ_t^{in} or χ_t^{out} can always be assigned the value 0. Since additional constraints can only deteriorate the optimal objective function value, this leads to the trigger variables acting as a proper indicator variables for the position of the car in most situations, that is, the reverse implications in (15) and (16) are likely to also hold.

Finally, we can strengthen the linear relaxation by adding constraints

$$\chi_t^{\text{in}} + \chi_t^{\text{out}} \geq 1 \quad \forall t \in T. \tag{20}$$

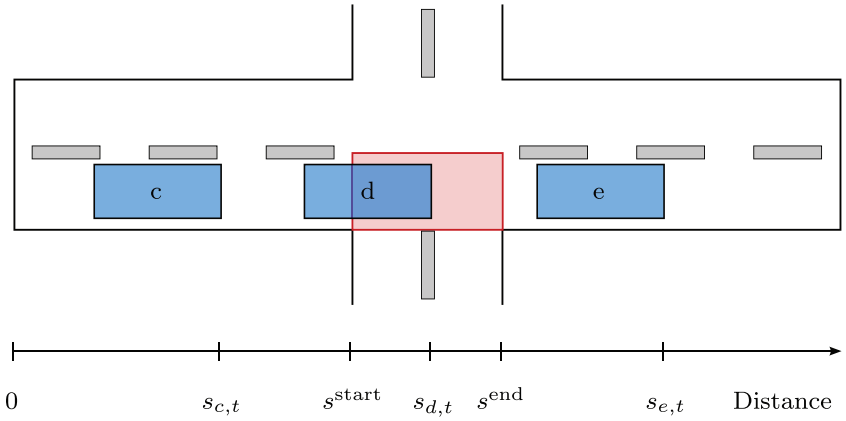

FIGURE 1 Three cars c, d, e driving on a lane in the network with red intersection area. We have $(\chi_t^{\text{in}}, \chi_t^{\text{out}}) = (0, 1)$ for car c, $(\chi_t^{\text{in}}, \chi_t^{\text{out}}) = (1, 1)$ for car d and $(\chi_t^{\text{in}}, \chi_t^{\text{out}}) = (1, 0)$ for car e

Traffic light trigger variables χ_t can be shared among all cars driving towards the same traffic light. Only the binary variables χ_t^{in} and χ_t^{out} have to exist for every pair of car and traffic light. Figure 1 shows the three main configurations of trigger variables for three different car positions. Also the intersection area for the lane the cars are driving on is visualized.

2.3 | Collision prevention on lanes

An essential part of modeling traffic at intersections is preventing collisions between cars. There are two types of possible collision situations we have to address in our modeling: first, we have to make sure that vehicles driving on the same lane do not collide, and second, we have to prevent collisions inside the intersection area, where vehicles from different lanes have to interact with each other. The second type is handled by traffic lights as has been described in Section 2.2. In order to prevent collisions of cars on the same lane we have to make sure that all cars keep a safety distance to their predecessors. Due to possible turning we need to distinguish between two cases: before and after crossing the intersection.

We regard the set of relevant predecessors of a car c driving on the same lane and introduce it as C_c^{pred}. The idea is to introduce constraints of the form

$$s_{c',t} - s_{c,t} \geq l_{c'} + g_c \quad \forall c \in C,\ c' \in C_c^{\text{pred}},\ t \in T_c, \tag{21}$$

where $l_{c'}$ denotes the length of car c' and g_c is the safety gap maintained by c to cars driving in front of c in the same lane. As we are considering networks with single lanes without overtaking maneuvers, each car has only one other car to watch out for, namely its direct predecessor. However, constraint (21) is only valid if both c and c' have the same destination. Otherwise the successor–predecessor relation will change after turning and we need variations of (21) that are disabled after one car has crossed the intersection. Also, we do not know the new predecessor of c after the intersection and hence will add binary variables that encode the crossing order of cars that drive on the same lane after crossing the intersection. For g_c we use a relatively small constant safety gap in this work since collision avoidance will be ensured by the central controller. For simulating human traffic, a non-constant safety gap is often chosen, motivated by the time to collision and depending on, for example, the velocities of c and c', typical reaction times and typical decelerations that drivers are willing to use (see, e.g., [20, Chapter 4]). Such would also be possible in our model, by replacing g_c by a velocity-dependent term.

2.3.1 | Collision prevention before crossing the intersection

If the car has not yet crossed the intersection, we can identify a unique direct predecessor $pred(c)$ of each car $c \in C$. Note, that the set of all cars C can be partitioned into the set C^{str} of cars going straight and the set C^{turn} of turning cars. We introduce constraints of one of the following forms depending on the turning behavior of the vehicles c and $pred(c)$:

- If both c and $pred(c)$ have the same destination, we can use (21) with $c' = pred(c)$.
- If c and $pred(c)$ have different destinations, we use big-M constraints

$$s_{pred(c),t} - s_{c,t} + \left(1 - \chi_{pred(c),t}^{\text{out}}\right) \cdot M \geq l_{pred(c)} + g_c \quad \forall t \in T_c. \tag{22}$$

Due to (16), the leave-trigger variable $\chi_{pred(c),t}^{\text{out}}$ takes the value of 1 if $pred(c)$ has not fully crossed the intersection at time point t (i.e., if $s_{pred(c),t} < S^{end}$), hence enforcing the required safety distance. Furthermore, it can always be set to 0 for $s_{pred(c),t} \geq S^{end}$ and hence the big-M term guarantees that the inequalities can always be satisfied if the car has already

crossed the intersection for sufficiently large M (one may use the longest possible covered distance until timepoint t, i.e., the length of the path which arises if the car would have driven with maximum velocity until timepoint t).

2.3.2 | Turning and collision prevention after crossing the intersection

In the case that cars have crossed the intersection the difficulty arises that the successor–predecessor relation changes and the order in which the cars cross the intersection is not known beforehand. Predecessors can come from different lanes when turning is involved.

To model the turning behavior we introduce new binary variables $O_{c,c'}$ for each pair of cars (c, c') that drive on different lanes before but on the same lane right after crossing the intersection. It encodes the crossing order as follows:

$$O_{c,c'} = \begin{cases} 0, & \text{if } c \text{ crosses before } c' \\ 1, & \text{if } c \text{ crosses after } c'. \end{cases} \tag{23}$$

Consequently, the variables $O_{c,c'}$ and $O_{c',c}$ have to satisfy

$$O_{c,c'} + O_{c',c} = 1. \tag{24}$$

With this we can now formulate the collision prevention constraints after crossing the intersection for cars c, c' as above:

$$s_{c,t} - s_{c',t} + (1 - \chi^{\text{in}}_{c,t} + O_{c,c'}) \cdot M \geq l_c + g_{c'} + \delta \quad \forall t \in T_c \cap T_{c'}, \tag{25}$$

$$s_{c',t} - s_{c,t} + (1 - \chi^{\text{in}}_{c',t} + O_{c',c}) \cdot M \geq l_{c'} + g_c + \delta \quad \forall t \in T_c \cap T_{c'}. \tag{26}$$

Equation (25) models the case where car c crosses before c', in which case c' is required to respect the safety distance requirement if c already entered the intersection area ($\chi^{\text{in}}_{c,t} = 1$, see (16)). Otherwise it can be easily satisfied thanks to big-M. Similarly, (26) is activated only if c' crosses before c and has already entered the intersection area. The adjustment parameter δ is added to project the distances of the vehicles onto the new destination lane after crossing the intersection. It depends on the length of their turning trajectories and the width of the intersection area.

Finally, the following constraints maintain the predecessor–successor relation between vehicles starting from the same lane and going to the same destination even after turning:

$$s_{PRE(c),t} - s_{c,t} \geq l_{PRE(c)} + g_c \quad \forall c \in C,\ t \in T_c, \tag{27}$$

where $PRE(c)$ is the *predecessor with the same destination* as car c. An example is shown in Figure 2. Here, vehicle c_1 turns left, c_2 goes straight and c_3 turns left, so $PRE(c_3) = c_1$. Note, that constraints (21) for the case that car c and its direct predecessor $pred(c)$ have the same destination are included in (27) with $PRE(c) = pred(c)$. Furthermore, Figure 2 demonstrates how to choose the adjustment parameter δ for vehicles turning left.

2.4 | Objective function

As we are looking for an optimal traffic flow of multiple cars on a fixed time horizon, we have to decide on a suitable objective function for this purpose. Optimal traffic flow could mean that one wants to reduce the overall traveling time of all cars for reaching their destination. As the time horizon is fixed, minimizing traveling time for a certain route is similar to maximizing the covered distance in the end of the horizon in our scenario. Therefore, we maximize the sum of the driven distances of all cars at the last time step N:

$$\max \sum_{c \in C} s_{c,N}. \tag{28}$$

In fact, we can show—under relatively mild assumptions which hold for our instances—that maximizing the total covered distance leads to a minimization of travel time, and with that automatically also a minimization of waiting time:

Lemma 1. *Let $s^* \in \mathbb{R}^{C,N}$ be an optimal trajectory maximizing objective function (28) on a finite horizon and let $\bar{v} > 0$ be the maximum allowed velocity for all vehicles $c \in C$. Let $s_I > 0$ be any distance that allows every vehicle to cross the intersection and reach maximum velocity at s_I. Let $t^* \in \mathbb{R}^C$ be the vector of times it takes for each vehicle to reach s_I according to s^*.*
Then t^* is minimal among all feasible trajectories, that is, any optimal solution with respect to total driven distance also optimizes travel time.

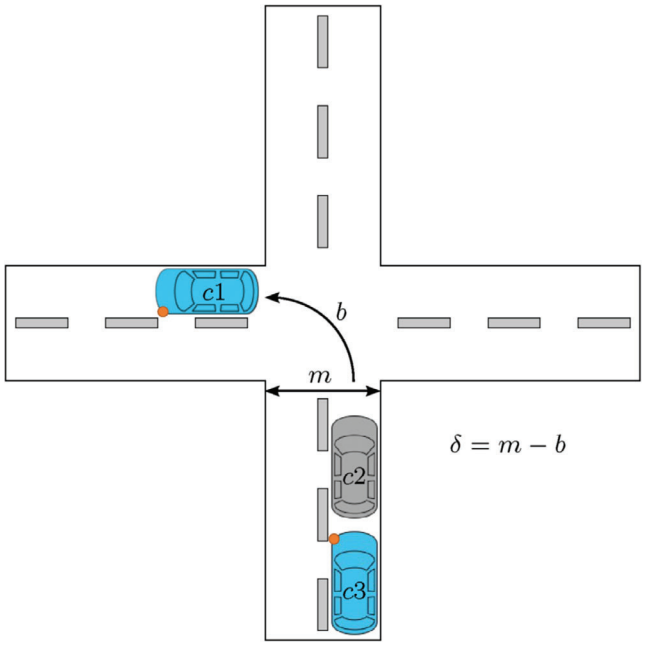

FIGURE 2 Visualization of the concept of the *predecessor with the same destination* and choosing the adjustment parameter

Proof. Let $f^* = f_I^* + f_R^*$ be the objective value of solution s^*, where $f_I^* = |C| \cdot s_I$ denotes the total distance to reach s_I and f_R^* denotes the total distance until time N, that is, the total distance driven after passing s_I till the end of the considered time horizon. Clearly, f_R^* is achieved when all vehicles have reached maximum velocity $\bar{v}$ at position s_I (which is always possible due to the choice of s_I) and continue to drive at maximum velocity till the end. Now assume there exists $\tilde{t} \in \mathbb{R}^C$ with

$$\sum_{c \in C} \tilde{t}_c < \sum_{c \in C} t_c^*.$$

Therefore, the total time remaining until N is

$$\sum_{c \in C} (N - \tilde{t}_c) > \sum_{c \in C} (N - t_c^*).$$

By extrapolating the trajectory belonging to $\tilde{t}$ until time N with all vehicles continuing to drive with maximum velocity, we obtain a feasible solution $\tilde{s}$ with

$$\begin{aligned} \tilde{f} &= \tilde{f}_I + \tilde{f}_R = f_I^* + \tilde{f}_R = f_I^* + \bar{v} \sum_{c \in C} (N - \tilde{t}_c) > f_I^* + \bar{v} \sum_{c \in C} (N - t_c^*) \\ &= f_I^* + f_R^* = f^*, \end{aligned}$$

contrary to f^* being optimal. ∎

Thinking about economical issues one could also try to minimize the overall emissions. As the presented model does not include exhaust rates or something similar, we can approximate this with the car's squared acceleration:

$$\min \sum_{\substack{c \in C, \\ t \in T}} a_{c,t}^2. \tag{29}$$

Note that this objective is nonlinear while the rest of the model is an MILP so far.

Our primary goal is to optimize the traffic flow. Only looking at objective (28), though, we observe that some vehicles do drive quite emission inefficiently in front of the intersection in cases in which it is foreseeable that they cannot make it across the intersection during the next green phase. For instance, the objective value would not change if a vehicle slowly approaches the intersection with a constant speed or performs several starts and stops as long as it reaches and crosses the intersection at the same time, but the emission values would be a lot higher in the latter case. It is therefore necessary to consider both, optimizing traffic flow and reducing emissions. The standard approach would be to unify the two objectives into a single multiobjective function of the form

$$\max \; w_1 \sum_{c \in C} s_{c,N} - w_2 \sum_{\substack{c \in C, \\ t \in T}} a_{c,t}^2 \tag{30}$$

as a weighted sum of both objectives. By adjusting the weights one explores the Pareto-optimal points, that is, solutions with the property that none of the two individual criteria can be improved while at least maintaining the other. We tackle this problem with a slightly different view: we set our primary goal to be the optimization of overall traffic flow, and from all optimal solutions in regard to that objective we would like to obtain the one which is best in terms of emissions. This two-step approach has two advantages: first, we avoid introducing a nonlinear term in the MILP model, which would make it a lot harder to solve. Second, after we obtain the best objective value in terms of traffic flow, we can fix all binary variables and solve the model again with the objective (29), effectively only solving a quadratic program (QP) in the second step. By fixing the binary variables, the order and times in which the vehicles cross the intersection remain unchanged, and only the driving behavior before and after crossing the intersection are adjusted to be more emission efficient. Briefly summarized, the steps are:

1. Solve MILP with objective function (28).
2. Change the objective function to (29).
   Add constraint
   $$\sum_{c\in C} s_{c,N} \geq f^* - \varepsilon$$
   to the model, where f^* is the objective value of step 1 and ε small.
   Fix all binary variables.
3. Solve the resulting QP.

2.5 | Summary of model and assumptions

For convenience, we list all constraints describing the passage of multiple vehicles over traffic light regulated intersections below, with no indices omitted. We refer to the resulting MILP (of step 1) as *global-MILP*. Note that also more complex networks than the rather simple one which served for introducing the model can be represented. For ease of notation, we introduce the set of traffic lights, which a car c passes during its traversal of the network as TL_c. Before we state the complete MILP, we list important assumptions we make regarding the model:

1. The time horizon T and the set of C of vehicles is finite.
2. The speed limit $\overline{v}$ is low, such that friction terms can be neglected. Also, the discretization step length $\frac{1}{dt}$ is chosen such that no car can pass the conflict zone of an intersection during a single time step.
3. All cars are controlled centrally.
4. We have full information on all traffic participants, which includes arrival times $t_{\text{init},c}$, initial velocities $v_{\text{init},c}$, and destinations.
5. We have error-free realization of the central controls. Hence, no unforeseen collisions can occur.

The complete MILP is then stated as follows:

$$\max_{\substack{s,v,a,\overline{y},\underline{y},\\ \chi,\chi^{\text{in}},\chi^{\text{out}},O}} \sum_{c\in C} s_{c,N}$$

s.t.	(2) – (10),	(motion model)
	(11), (12) – (14),	(traffic light constraints)
	(17) – (20), $\quad \forall c \in C,\ tl \in TL_c,\ t \in T_c,$	
	(22), $\quad \forall c \in C : dest(c) \neq dest(pred(c)),$	(collision prevention)
	(24), (25), $\quad \forall c, c' \in C : O_{c,c'}$ is defined,	
	(27).	

3 | EXPERIMENTAL SETTING

The performance of an intersection is influenced by two factors: the operation of the traffic lights, and the behavior of autonomous and/or human drivers. In this section, we want to describe the experimental setting we use to investigate and quantify the potential of improvements for different scenarios, such as modifying traffic-light regulations or not imposing any rules on traffic lights at all. The results allow us to determine the capacity of a road network under different conditions, which can serve as a benchmark for decentralized and heuristic approaches.

First, we introduce the four scenarios we consider:

- real-world traffic with a fixed traffic light scheme;
- all vehicles are autonomous, traffic lights have to follow a predefined, fixed scheme;
- all vehicles are autonomous, traffic lights have to ensure minimum lengths of green and red phases;
- all vehicles are autonomous, there are no restrictions on the switching schemes of the traffic lights.

For simplicity, we denote the four different scenarios as (RW), (FIX), (MIN), and (FREE), respectively.

Before we discuss the results of the experiments in Section 4, we define a consistent experimental setting, present the used traffic-simulation software, and consider the representation of real-world traffic in the simulation.

3.1 | Traffic simulation software

In order to analyze and rate the effects on traffic, it is necessary to realistically represent the motion of cars and the behavior of human drivers. Furthermore, the chosen software should allow control of the movements of all cars on the road and the traffic light's signal states in fine time steps. Hence, a microscopic traffic simulation software seems appropriate for our purposes. They allow the simulation of single cars and other entities in the network according to *car-following-models* that model the individual behavior of cars depending on the movement of their respective predecessor. Common examples from the literature are the models of Krauß [20], and the IDM by Treiber and Kesting, cf. [17, 38].

We use the *SUMO* (*Simulation of Urban MObility*) software framework, cf. [19], to analyze and visualize the computed results. SUMO is a free and open-source traffic-simulation suite which allows modeling of intermodal traffic systems including road vehicles, public transport, and pedestrians. It comes with a variety of possibilities for evaluating the simulated traffic. These are, for example, CO_2-emissions and fuel consumption according to the German Federal Environment Agency [39]. The behavior of traffic lights and cars can be accessed via *TraCI* (*Traffic Control Interface*) which allows to retrieve values of simulated objects and to manipulate their behavior online.

Furthermore, SUMO implements two traffic signal control approaches which allow the user to dynamically change the length of phases depending on the incoming traffic. The first approach are *actuated traffic lights* based on time gaps. The traffic phases are prolonged whenever a continuous stream of traffic is detected, and switches when there is a sufficient time gap between two successive vehicles. The second approach is the *delay-based control*. Here, a phase prolongation is triggered based on the accumulated time loss of vehicles. If the time loss exceeds a predefined value, the corresponding green phase is prolongated if active [28, 29]. Another algorithm, *AGLOSA* [6], which uses V2I communication to alternately optimize the signal plan and the vehicle trajectories, has been implemented via SUMO's TraCI, but unfortunately is not publicly available. Therefore, we limit ourselves to the two approaches which are already implemented in SUMO and compare them in Section 4.2 to solutions of the global-MILP.

3.2 | Test instances

All of the testing instances are processed on the simple network which is depicted in Figure 3. It consists of a single intersection of two roads, each with one lane in either direction. All lanes have a width of 3.5 m and a stretch of 200 m of road is added in each direction from the intersection.

The fixed switching schemes of the traffic lights include a green phase and a red phase for all traffic lights of the intersection. In the real-world case a short red-amber phase is included before the green phase. Each cycle consists of four succeeding and equal phases for each lane in clockwise order. For the (MIN) case, we demand a minimal duration on the green phase. In contrast to the fixed case, the green phases can last longer and the starting times and order of the phases are not predefined. To be comparable, the minimum duration of the green phase is set to the length of the green phase of the fixed case. We also demand the same minimum length of green phases for the two adaptive traffic signal approaches which are available in SUMO. As mentioned before, there are no restrictions in the (FREE) case.

The arrival time of each car is fixed for each scenario and is randomly chosen according to the following principle: a mean rate of cars per lane and minute for a certain amount of minutes is fixed. The actual number of cars for each minute is randomly distributed according to a Poisson distribution, which according to Gallager [11] is suitable for generating traffic-related data. Specific arrival times are distributed equidistantly over the minute. We consider four different traffic densities. For each density five random instances are generated and processed for the four scenarios. The evaluated parameters are geometric means of all five instances and apply for single cars. For all methods, we set the discretization step to $dt = 0.5$ s. The physical bounds on the motion of the cars are chosen similarly for each method according to Table 1.

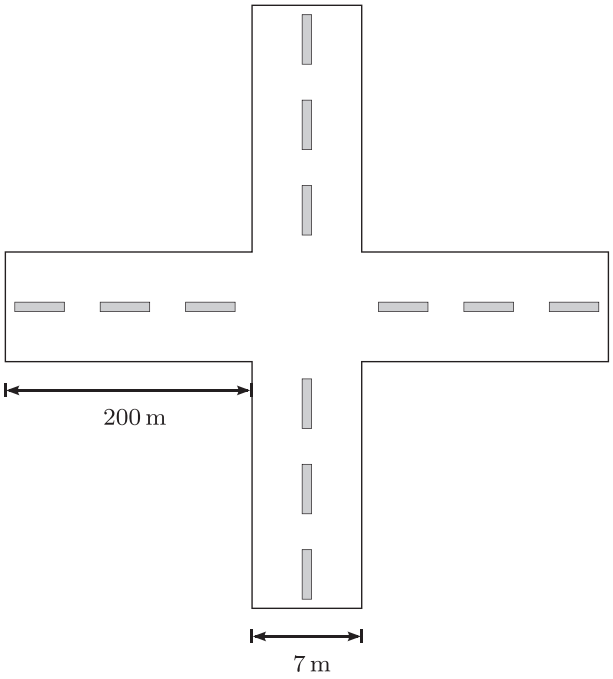

FIGURE 3 Layout of the network used for numerical investigation

TABLE 1 Bounds on the states of the vehicles which are equal for cars and scenarios

	Value	Description
$\underline{v}_c$	0	Minimum velocity in m/s
$\overline{v}_c$	15.27	Maximum velocity in m/s
$\underline{a}_c$	−7.5	Minimum acceleration in m/s^2
$\overline{a}_c$	2.9	Maximum acceleration in m/s^2
$\underline{j}_c$	−3	Minimum jerk in m/s^3
$\overline{j}_c$	3	Maximum jerk in m/s^3
l_c	4.3	Length of the car in m
g_c	2.5	Security gap of the car in m

For the computed traffic of the four scenarios we use following quality measures:

- the value of the objective function, meaning the accumulated driven distance of all cars;
- the mean *travel time* and *waiting time* of all cars in the network. While travel time measures the time it takes for each car to traverse the network, the waiting time measures the difference between travel time and theoretical time for an unobstructed traversal of the network. Both values are suitable for indicating the quality of traffic flow according to Forschungsgesellschaft für Straßen- und Verkehrswesen e.V. [7].
- the mean simulated *fuel consumption* and CO_2 *emissions* of all cars in the network. We also refer to these parameters as *environmental parameters*.

All computations were performed on a server with 32 cores (Intel(R) Xeon(R) CPU E5-2640 v3 @ 2.60 GHz) and 31 GB of RAM, running Debian GNU/Linux 10. CPLEX V12.9 serves as the MILP-solver for all optimization problems occurring here. Preliminary experiments have shown that the solver performed better without presolve during preprocessing, which is why we disabled it for our computations. Finally, SUMO is used in version 1.1.0.

3.3 | Real-world traffic

A crucial part for analyzing the effects on traffic is to simulate real-world traffic appropriately. Usually, traffic is simulated in SUMO using car-following models. By default, the model by Krauß [20] is enabled which provides different parameters to adapt the behavior of cars in the simulation. That way, different types of vehicles such as passenger cars, motorcycles, trucks, and busses can be modeled. Aside from the parameters shown in Table 1, additional parameters like the driver's imperfection or

TABLE 2 Adjustable parameters for the default car-following model in SUMO with used values

Parameter	Value	Description
accel	2.9	Acceleration ability
decel	−7.5	Deceleration ability
sigma	0.5	Driver imperfection ∈ [0, 1]
tau	1.0	Reaction time
minGap	2.5	Gap to front vehicle if halting

reaction time influence the driving behavior. In our simulation we use the standard passenger car. Table 2 shows the adjustable parameters and used values for each of them. Later computations about emissions also use the default model for passenger cars, and are based on the emission model descriptions HBEFA3 of the German Federal Environment Agency [39].

3.4 | Moving-horizon approach

As we will see in Section 4, computation times can be quite high when trying to solve the full MILP model. To cope with this problem we apply a moving-horizon framework. If the time span of the MILP is large, solving the entire optimization problem results in a large optimization model with many constraints and variables. If the problem can be split into smaller time periods which are coupled subsequently, the resulting—much smaller—subproblems can be solved progressively. This section will give a brief description of the moving-horizon approach, for more details we refer to [8, 31].

The general idea is to not solve the MILP model on the whole time horizon $\mathcal{T} = [0, t_f]$, but instead repeatedly on shorter *prediction horizons* $\mathcal{T}_i = [t_i, t_{i+n}]$ which move forward in time. Figure 4 visualizes the general concept for the continuous case, but it can easily be applied to the discrete case. At sampling time t_i we solve the problem on the prediction horizon $\mathcal{T}_i = [t_i, t_{i+n}]$ starting with the initial condition $x(t_i) = \hat{x}(t_i)$, yielding an optimal predicted state trajectory x^*. We apply the first part of the trajectory until t_{i+1} to our final solution. After that, we shift our time horizon by the *sampling period* $h := t_{i+1} - t_i$ and repeat the process for a new initial state observation $\hat{x}(t_{i+1})$. That way we progressively construct the solution for the whole time horizon $\mathcal{T} = [0, t_f]$.

4 | EXPERIMENTAL RESULTS

In this section, we want to investigate and quantify the potential of improvements for the different scenarios we defined in the previous section. We first give some computational evidence on the performance of the global-MILP on these different scenarios considering two dimensions: performance of an MILP-solver on the testing data and resulting traffic flow according to traffic simulations. In the second part we use the results of the centralized approach as a benchmark to determine the quality of obtained solutions from the moving-horizon approach.

4.1 | Experimental results on the global-MILP

In this section, we discuss the quality of solutions obtained by the global-MILP in terms of the aforementioned quality measures. We first investigate the performance of the solution process, which is depicted in Table 3.

The table lists the runtimes and objective function values (for the MILP *maximization of driven distance*) for the three scenarios (FIX), (MIN), and (FREE) for different traffic densities, averaged over five testing instances each. The column *MILP* shows the computation times for solving the MILP, while the column *QP* shows the time for solving the additional QP problems minimizing the sum of squared accelerations. The column *total* sums up both.

The computation times for the MILP as well as the QP increase with a higher density of cars, but are still manageable for the (FIX) and (FREE) case, ranging from around 1 s for the smallest density up to around 15 s for the MILP and 10 s for the QP for the highest density. The MILP problem gets significantly harder when minimal green and red times, that is, min-up-down constraints on the binary variables controlling the traffic lights, are added in the (MIN) case, though. While in the smallest case this leads to a computation time average of 111 s, it goes up to 19,000 s for the second highest density, and 3 out of 5 instances could not be solved to optimality within a 10 h time frame for the highest density. Since all the integer variables are fixed when solving the additional QP, runtimes here behave similarly to the (FIX) case.

Looking at the objective values of the MILPs, as expected, the values (total driven distance) increase when traffic lights are less regulated and have more freedom in controlling the traffic. This increase tends to be larger the higher the density is.

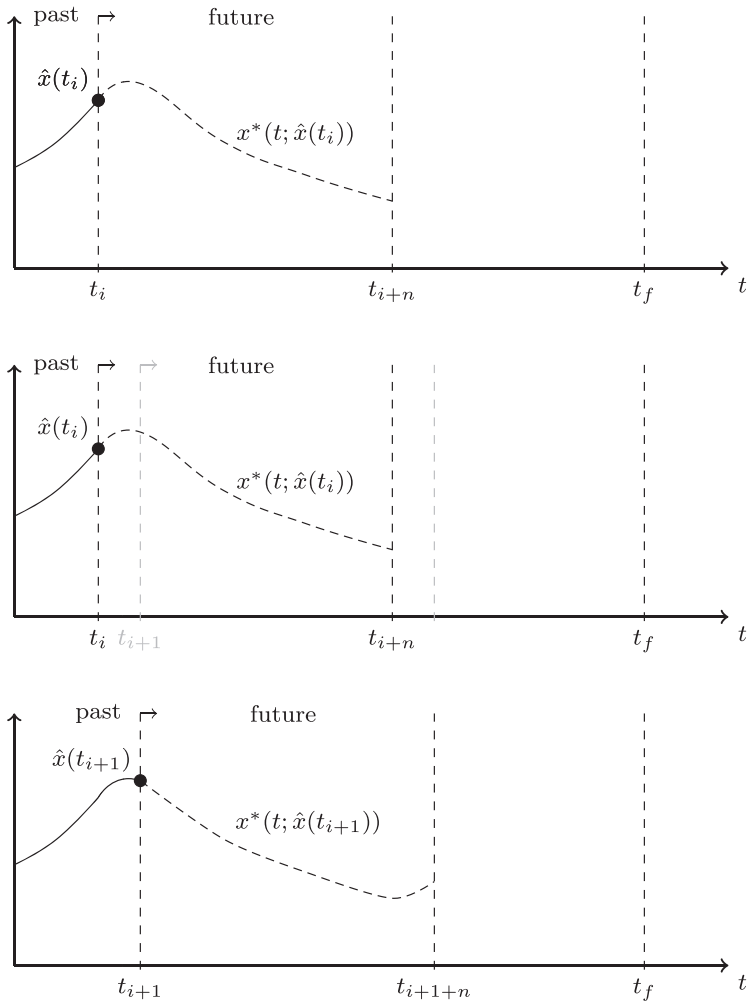

FIGURE 4 Illustration of the moving-horizon approach

Considering the quality of the resulting traffic, we now concentrate on the parameters travel time, waiting time, CO_2-emissions, and fuel consumption. In order to retrieve these values, the default driving behavior was disabled in SUMO and the optimal solutions computed by the model were adopted. Going from (RW) to (FIX) to (MIN) and lastly to (FREE), the degree of freedom granted to the optimization procedure increases. The focus of this study is to determine how this increase is reflected in the quality of results for overall traffic flow as well as the environmental parameters. To this end, the offline-calculated solutions via CPLEX are transferred into SUMO. The Python interface TraCI allows us to control the motion of all cars in each time step. Thus, we can retrieve the parameters of interest from the solutions of the MILP. Table 4 shows the relevant measurements. Throughout all the problem instances we observe an improvement in all four parameters when we increase the degree of optimization. Largest improvements are achieved by going from the (RW) case to the (FIX) case, where we leave the traffic lights as they were, but optimize the traversal of the cars throughout the network, and going from the (MIN) case to the (FREE) case by removing all restricting rules on the traffic lights. Looking at the highest density traffic in more detail, we achieve a decrease in waiting times of about 44.47% with (FIX), 49.59% with (MIN), and 99.05% with (FREE) compared to the (RW) case. The travel times per vehicle decrease by 32.29%, 34.61%, and 53.63%. Although we were primarily optimizing in terms of overall traffic flow, and considered emissions in a second step by solving the QP, we still observe a significant improvement regarding the environmental parameters. For the fuel consumption and CO_2-emissions, we register a decrease of 13.91%, 16.06%, 39.91% and 13.89%, 16.04%, 39.90%, respectively. Although smaller, improvements were prominent even on traffic with lower densities.

4.2 | Comparison to SUMO's traffic signal controls

SUMO implements two adaptive traffic signal controls that can prolongate green phases based on incoming traffic. One can set a minimal and maximal duration of the green phase. For comparison reasons we set the minimal duration to 10 s and leave the maximal duration open as we have demanded for previous computations. Further parameters are shown in Table 5.

TABLE 3 Measurements for traffic with different densities and scope of optimization

Density (cars/min)	T (s)	dt (s)	L (s)	Computation times			Objective value
				Total (s)	MILP (s)	QP (s)	MILP (m)
20.95	60	0.5	10				
Fixed traffic lights				24.41	13.76	10.65	28209.2
Regulated traffic lights				32533.80(2)	32524.10(2)	9.71	29173.1(2)
Free traffic lights				18.42	15.29	3.13	38468.4
15.06	60	0.5	10				
Fixed traffic lights				9.38	4.57	4.80	20578.6
Regulated traffic lights				19079.54	19075.50	4.04	21451.9
Free traffic lights				10.91	9.26	1.65	27627.8
9.5	60	0.5	10				
Fixed traffic lights				4.28	2.25	2.03	12891.9
Regulated traffic lights				1128.13	1126.30	1.83	14056.7
Free traffic lights				3.01	2.09	0.92	17392.8
5.11	60	0.5	10				
Fixed traffic lights				1.73	0.89	0.84	7230.3
Regulated traffic lights				111.94	111.19	0.75	7892.6
Free traffic lights				1.44	1.01	0.43	9353.2

Note: Measurements are geometric means per vehicle of five testing instances. If only a subset of instances has been solved, the number of solved instances is given in brackets. Means were taken over all five instances; computation times for unsolved instances are set to the time limit of 10 h.

TABLE 4 Minimizing squared acceleration after maximizing driven distance

Density (cars/min)	T (s)	dt (s)	L (s)	Waiting time (s)	Travel time (s)	Fuel (l/100 km)	CO_2 (g/km)
20.95	60	0.5	10				
Real-world simulation				14.67	57.89	10.67	248.29
Fixed traffic lights				8.14	39.20	9.19	213.80
Regulated traffic lights				7.39	37.86	8.96	208.47
Free traffic lights				0.14	26.84	6.41	149.23
15.06	60	0.5	10				
Real-world simulation				12.58	50.20	10.56	245.59
Fixed traffic lights				7.78	38.57	8.81	205.06
Regulated traffic lights				6.84	36.89	8.61	200.21
Free traffic lights				0.12	26.84	6.51	151.42
9.5	60	0.5	10				
Real-world simulation				10.36	44.24	10.36	241.04
Fixed traffic lights				7.83	38.75	8.59	199.84
Regulated traffic lights				5.83	35.12	8.14	189.37
Free traffic lights				0.08	26.79	6.55	152.30
5.11	60	0.5	10				
Real-world simulation				9.03	40.62	10.23	237.95
Fixed traffic lights				6.85	36.73	8.03	186.91
Regulated traffic lights				4.66	33.36	7.71	179.44
Free traffic lights				0.10	26.81	6.59	153.21

Note: Measurements for traffic with different densities and scope of optimization. Measurements are geometric means per vehicle of five testing instances.

Table 6 shows the retrieved quality measures for the two traffic signal controls. Here, *actuated control* stands for the traffic signal control based on time gaps, while the *delay-based* control is based on time loss. For comparison we also again show the results for real-world simulation with a fixed traffic light cycle as well as the values for the (MIN) case from the optimization from Tables 3 and 4. In terms of waiting time and travel time, of the three SUMO-based simulations the actuated control performs slightly better than the other two. Regarding fuel consumption and CO_2-emissions, the difference between the three simulations is negligible, without being able to tell a clear best method. The optimization-based method performs best, roughly cutting the

TABLE 5 Adjustable parameters for the adaptive signal controls in SUMO with used values

Parameter	Value	Description
max-gap	1.0	Maximum time gap between successive vehicle (s)
minDur	10	Lower bound on the phase length (s)
maxDur	60	Upper bound on the phase length (s)
detectorRange	150	Upstream detection range (m)
inTimeLoss	1.0	Minimum time loss for triggering phase prolongation (s)
minDur	10	Lower bound on the phase length (s)
maxDur	60	Upper bound on the phase length (s)

Note: On top are the parameters for the actuated control, on the bottom the parameters for the delay-based control.

TABLE 6 Comparison to SUMO's traffic signal controls

Density (cars/min)	T (s)	dt (s)	L (s)	Waiting time (s)	Travel time (s)	Fuel (l/100 km)	CO_2 (g/km)
20.95	60	0.5	10				
Real-world simulation				14.67	57.89	10.67	248.29
Actuated control				14.15	55.99	10.76	250.24
Delay-based control				14.25	56.34	10.94	254.50
Regulated traffic lights				7.39	37.86	8.96	208.47
15.06	60	0.5	10				
Real-world simulation				12.58	50.20	10.56	245.59
Actuated control				12.14	49.14	10.42	242.38
Delay-based control				12.28	49.31	10.68	248.43
Regulated traffic lights				6.84	36.89	8.61	200.21
9.5	60	0.5	10				
Real-world simulation				10.36	44.24	10.36	241.04
Actuated control				10.31	44.17	10.25	238.50
Delay-based control				10.34	44.17	10.28	239.25
Regulated traffic lights				5.83	35.12	8.14	189.37
5.11	60	0.5	10				
Real-world simulation				9.03	40.62	10.23	237.95
Actuated control				8.90	40.39	10.17	236.52
Delay-based control				9.31	41.21	10.42	242.30
Regulated traffic lights				4.66	33.36	7.71	179.44

Note: Minimizing squared acceleration after maximizing driven distance. Measurements for traffic with different densities and scope of optimization. Measurements are geometric means per vehicle of five testing instances.

waiting time in half, while also reducing the fuel consumption and CO_2-emissions. Even the more restrictive optimization with fixed traffic lights from the previous section performs considerably better.

4.3 | Experimental results on the moving-horizon approach

As we have seen, computation times exceed real-time requirements. We also consider a moving-horizon approach derived from our centralized model. We compare its performance and obtained solutions to the centralized approach, showcasing an example use of the latter as a benchmark.

First, we investigate the runtimes and obtained objective values for solving the MILP. Here, we focus on the (MIN) case, where computation times are especially high. Table 7 shows the results, listing overall runtime, maximum time for one moving-horizon iteration, and the objective value, averaged over the same five problem instances. A more detailed breakdown into the used instances is shown in Appendix A. The prediction horizon was set to 20 s and the sampling period to 7.5 s.

As expected, computation times go down significantly throughout all four density levels, when applying the moving-horizon framework. This reduction in computation time is most pronounced in the higher density cases, where we have a reduction in averages from over 32,000 s to about 271 s and over 19,000 s to about 166 s, respectively. But also in the smallest density case we still obtain an improvement from 111 to 21 s. Looking at the objective values, we observe that the obtained solutions are close to the globally optimal solutions, their gap being less than 3% for all density cases. In some instances even optimality is obtained,

TABLE 7 Comparison of computation time and objective value between moving-horizon and global-MILP

Density	T	dt	L	Moving-horizon			Global-MILP	
(cars/min)	(s)	(s)	(s)	Total (s)	Max (s)	Obj.	Total (s)	Obj.
20.95	60	0.5	10					
Regulated traffic lights				271.60	72.13	28551.2	32524.10(2)	29173.1(2)
15.06	60	0.5	10					
Regulated traffic lights				166.20	48.40	20893.5	19075.50	21451.9
9.5	60	0.5	10					
Regulated traffic lights				77.42	20.44	13736.7	1126.30	14056.7
5.11	60	0.5	10					
Regulated traffic lights				21.51	6.04	7770.0	111.19	7892.6

Note: Measurements for traffic with different densities. Measurements are geometric means per vehicle of five testing instances. The length of the prediction horizon $\mathcal{T}_i$ was set to 20 s and the sampling period h to 7.5 s. If only a subset of instances has been solved, the number of solved instances is given in brackets. Means were taken over all five instances; computation times for unsolved instances are set to the time limit of 10 h.

TABLE 8 Environmental parameters for the moving-horizon approach (mh)

Density	T	dt	L	Waiting time	Travel time	Fuel	CO_2
(cars/min)	(s)	(s)	(s)	(s)	(s)	(l/100 km)	(g/km)
20.95	60	0.5	10				
Regulated traffic lights				7.39	37.86	8.96	208.47
Regulated traffic lights (mh)				7.87	38.91	9.25	215.27
15.06	60	0.5	10				
Regulated traffic lights				6.84	36.89	8.61	200.21
Regulated traffic lights (mh)				7.44	38.11	8.74	203.28
9.5	60	0.5	10				
Regulated traffic lights				5.83	35.12	8.14	189.37
Regulated traffic lights (mh)				6.36	36.12	8.10	188.54
5.11	60	0.5	10				
Regulated traffic lights				4.66	33.36	7.71	179.44
Regulated traffic lights				5.03	33.98	7.35	170.90

Note: Minimizing squared acceleration after maximizing driven distance. Measurements for traffic with different densities and scope of optimization. Measurements are geometric means per vehicle of five testing instances.

see Appendix A. Note that all the solutions of the moving-horizon approach compare favorably to the optimal solutions of the (FIX) case (which could also be seen as a heuristic for the (MIN) case).

Although the time reductions and obtained objective values are promising, the maximum computation time per moving-horizon iteration in the higher density cases still exceeds the length of the sampling period and is thus too high for real-time use—in particular for the higher-density cases.

Next, we compare the results of the moving-horizon approach regarding the parameters waiting time, travel time, fuel consumption, and CO_2-emissions, which are depicted in Table 8. The moving-horizon approach leads to an increase in waiting time of less than 10% in the worst case, which amounts to less than a second difference compared to the central approach in all density cases. This increase in waiting time results in an increase of overall travel time of only about 3% in the worst case, which is around 1 s. Looking at the parameters fuel consumption and CO_2-emissions, we even observe cases where the moving-horizon approach has an improvement. Note that we primarily optimized over the total driven distance and reduce fuel consumption and CO_2-emissions in a second step. Overall, both approaches give similar results in terms of these two parameters.

4.4 | Discussion

For certain assumptions, our model provides globally optimal solutions for the maximal covered distance, which is shown in Lemma 1 to provide globally optimal solutions for travel and waiting times. Optimal solutions concerning fuel consumption and CO_2 emissions are not well defined, unfortunately, as they depend on the considered time horizon. If no boundary condition (all cars need to reach their target destination) is specified, the trivial lower bounds are 0 (no acceleration at all, depending on initial velocity and modeled friction). We provide a model and a methodology that makes it possible to balance the different objective

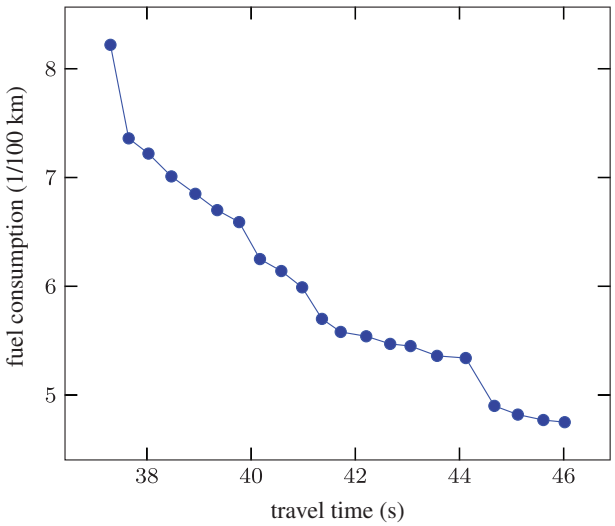

FIGURE 5 Approximation of the Pareto front for balancing travel time vs. fuel consumption for instance *small-5-fi* from Table A1

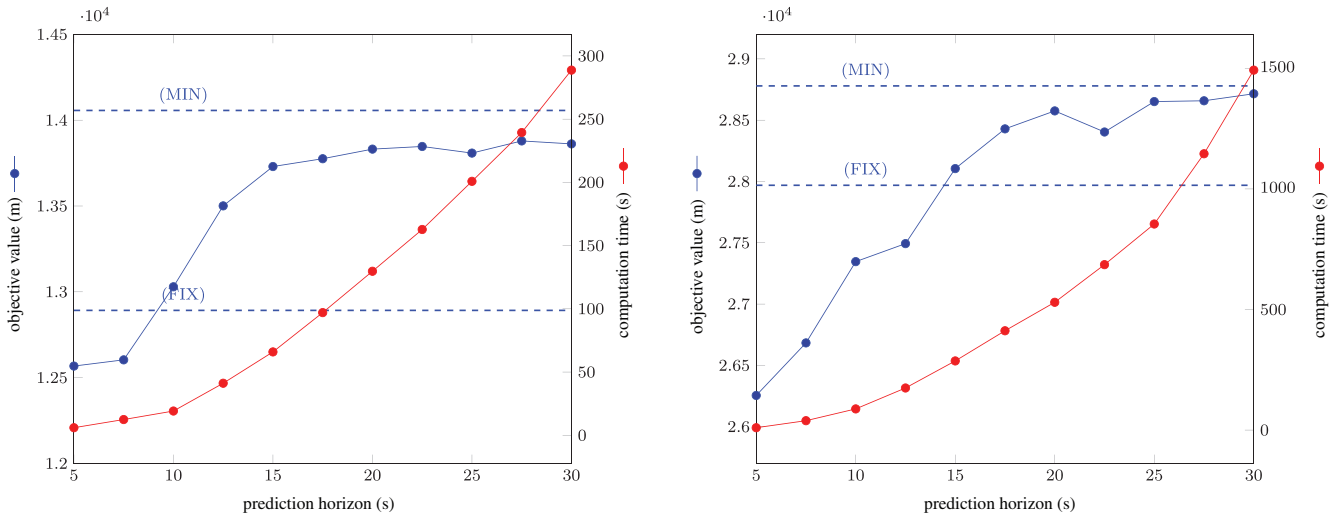

FIGURE 6 Influence of different prediction horizons on objective value and computation times for instances of density *medium* (left) and *veryhigh* (right). Sampling period is fixed to 2.5 s. Measurements are geometric means of five testing instances

functions against one another (via multiobjective optimization or simply specifying limits for some criteria as constraints). In Figure 5 one sees an approximation of a Pareto front for travel time versus fuel consumption for one particular problem instance.

In Table 6 we observed that the gap between solutions of SUMO's traffic signal control and the global-MILP is considerably large. The question arises, which factors contribute to that improvement. While both approaches adapt the switching of the traffic lights to react to incoming traffic, only the second one also optimizes the driving behavior of the cars. Making use of having full information, for example, when exactly a red traffic light will turn to green, cars adapt their speeds in advance to allow a smooth transition over the intersection which avoids unnecessary halting in front of the intersection. Considering only the optimization of the traffic lights as in SUMO's traffic signal control, they do not fully profit from the information available in a centralized setting. Our overall impression is that, while traffic-light regulations have a big impact, most potential for improvement for given regulations lies in the driving behavior rather than in the traffic light's switching times. Table 4 supports this assumption: optimizing driving behavior while keeping the traffic lights fixed, which is the case when we go from (RW) to (FIX), leads to a large improvement, whereas additionally optimizing the traffic lights, which is the case when we go from (FIX) to (MIN), results in a relatively small improvement. Furthermore, Table 8 suggests that the improvement is mainly due to sharing short-term information rather than due to planning far ahead in time.

In Figure 6 we analyze the influence of different prediction horizons in the range of 5–30 s on the objective value and computation time while the sampling period is fixed to 2.5 s. Full results are shown in Appendix A. Shorter prediction horizons tend to produce infeasible subproblems, since cars may approach halting cars or red traffic lights with a speed that does not allow to come to a halt in time for the chosen bounds on acceleration and jerk. Thus, a crash will inevitably happen, but only

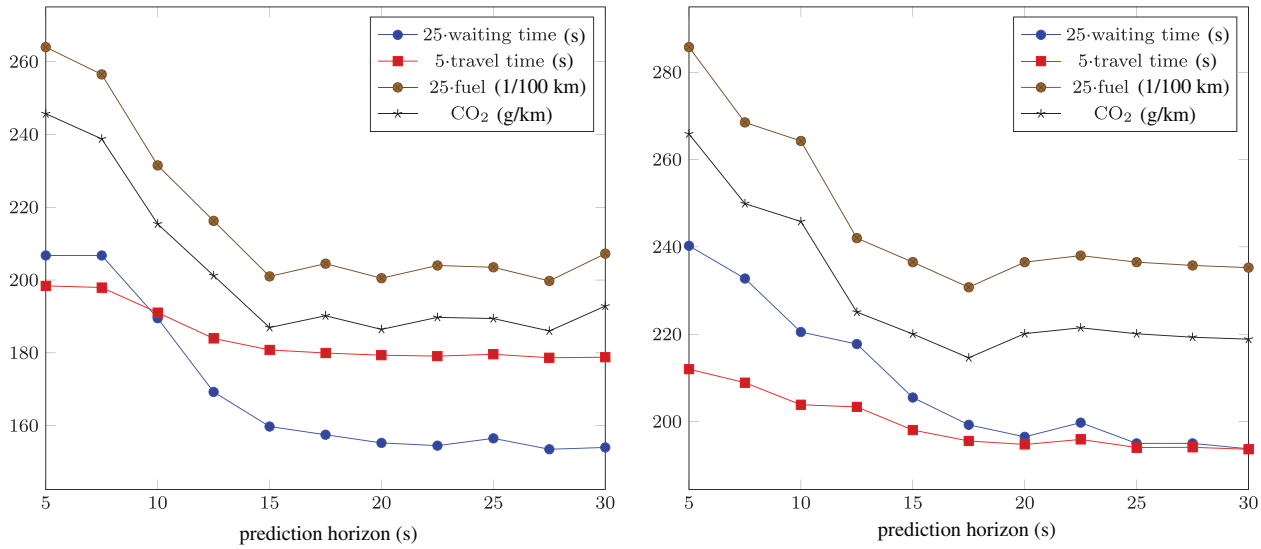

FIGURE 7 Influence of different prediction horizons on environmental parameters for instances of density *medium* (left) and *veryhigh* (right). Sampling period is fixed to 2.5 s. Measurements are geometric means of five testing instances

after the end of the prediction horizon. Additionally, we marked the objective values obtained from the global-MILP for fixed traffic lights as well as regulated traffic lights as a reference for evaluating solution quality. The latter represents the global optimum (or the best known bound), whereas the objective value of the problem with fixed traffic lights provides a cheap and fast feasible solution. With increasing prediction horizon we observe an increase in solution quality, but also in computation times. This is expected, since a longer prediction horizon allows the cars to look further into the future in order to, for example, react in advance to traffic light switches or incoming cars, but also results in a larger problem size which is reflected in higher computation times. By raising the prediction horizon, the objective value approaches the global optimum. It seems, though, that the curve flattens, meaning an increase in prediction horizon may only contribute to a small increase in solution quality. For the two considered problem cases we can improve the solution with fixed traffic lights by choosing a prediction horizon of at least 10 and 15 s, respectively. However, it is generally hard to predict the "optimal" length of the prediction horizon, considering also its effect on the computation time. Similar improvements can be observed for the environmental parameters in Figure 7. Since we are not primarily optimizing for fuel consumption and CO_2-emissions, we may observe some fluctuations, while waiting time and travel time behave rather monotonically.

An important contribution to faster and more energy-efficient driving comes from a predictive behavior, that is, decelerating ahead in time and accelerating such that critical bottlenecks (the traffic light intersections) can be crossed quickly. Solutions indicate that cars might even stop before the traffic lights and accelerate shortly before the traffic lights turn to green. These strategies were implemented in a simple controller called "Kreuzungslotse" (intersection pilot) [36]. Receiving only information about the future traffic light states, the controller acts on some simple driving strategies depending on the situation (e.g., existence of preceding cars, distance to traffic light and time to next traffic light switch) to plan ahead and compute a trajectory to cross the intersection. Despite the limited information, a significant improvement in traffic flow could be achieved.

5 | CONCLUSIONS

In this article, we introduced a novel MILP which models the movement of individual cars on a network of roads that intersect in multiple traffic-light controlled intersections and the switching scheme of traffic lights regulating the transit of cars. An advantage of the MILP is the presence of linear but realistic motion dynamics for each vehicle and the flexibility to model different traffic scenarios by modifying parameters such as traffic density, turning behavior and traffic-light regulations. Its solution by offline calculations yields an overall optimized traffic flow. Furthermore, by solving an additional QP we obtain traffic that is also energy efficient. Through simulations we analyze the influence of the aforementioned parameters on the overall traffic efficiency. Numerical results indicate that centrally optimized traffic leads to almost no waiting times (mean waiting times could be decreased by up to 99%) and a reduction in average fuel consumption of 39% in case of completely free traffic lights. However, also the more realistic case of controllable traffic lights that are bound to certain regulations on phase lengths leads to significant improvements in waiting times, fuel consumption and CO_2-emission when compared to simulated real-world traffic.

In the growing field of assisted and autonomous driving applications, the solutions of the MILP can serve as a benchmark for suboptimal but practically implementable algorithms in cars and infrastructural devices. The globally optimal solutions

computed are difficult to realize in a realistic setting. This is not only due to the relatively long solution times but also due to the fact that a resulting real-world system would be based on the premise that all cars are equipped with this system and bound to follow the system's advice.

We used the results from our centralized model to evaluate example heuristic approaches: SUMO's advanced intersection control features offer slight performance improvements over a fixed traffic light schedule while being very easy to implement in practice. However, there is still a lot of room for improvements, as a comparison with globally optimal solutions reveals. Solving our model in a moving-horizon framework allows us to come very close to the global optimum while solution times are not prohibitively large for real-time use. Still, some additional improvements are needed to speed up solution times, possibly by tuning the lengths of the prediction horizon $\mathcal{T}_i$ and the sampling period h, warmstarting iterations, or problem specific cutting planes or branching schemes.

Future research will involve further development of decentralized algorithms to find a good balance between solution quality and suitability for practical use. This work allows us to validate the effectiveness of such algorithms and the quality of its solutions. An important open question is the realistic incorporation of human drivers into our model formulation, allowing mixed-traffic scenarios involving both human drivers and centrally-controlled vehicles that can still be solved to global optimality.

ACKNOWLEDGMENTS

The authors would like to thank the Deutsche Forschungsgemeinschaft (DFG, German Research Foundation) for support within GRK 2297 MathCoRe. Additionally, this work was supported in part by Volkswagen Group Research and Group Strategy. We thank Rolf Findeisen, Johanna Bethge, Hannes Rewald, and Anton Savchenko for constructive discussions within the joint research project. Last but not least, we thank the anonymous reviewers for their helpful comments. Open access funding enabled and organized by Projekt DEAL.

DATA AVAILABILITY STATEMENT

The instances used for the computational study in this article are available on reasonable request.

ORCID

Maximilian Merkert https://orcid.org/0000-0002-7838-445X
Mirko Hahn https://orcid.org/0000-0002-2442-3978
Sebastian Sager https://orcid.org/0000-0002-0283-9075

REFERENCES

[1] H. Ahn and D. Del Vecchio, *Safety verification and control for collision avoidance at road intersections*, IEEE Trans. Automat. Contr. **63** (2018), no. 3, 630–642. https://doi.org/10.1109/TAC.2017.2729661
[2] G. Araniti, C. Campolo, M. Condoluci, A. Iera, and A. Molinaro, *LTE for vehicular networking: A survey*, IEEE Commun. Mag. **51** (2013), no. 1, 148–157.
[3] J. Bethge, R. Findeisen, D. Le, M. Merkert, R. H. S. Sager, A. Savchenko, and S. Sorgatz, *Mathematical optimization and machine learning for efficient urban traffic*, in *KoMSO success stories on mathematics in industry*, K.-H. Küfer, P. Maass, A. Milde, and V. Schulz, Eds., Springer, New York, NY, 2020.
[4] L. Chen and C. Englund, *Cooperative intersection management: A survey*, IEEE Trans. Intell. Transp. Syst. **17** (2016), no. 2, 570–586. https://doi.org/10.1109/TITS.2015.2471812
[5] K. Dresner and P. Stone, *A multiagent approach to autonomous intersection management*, J. Artif. Intell. Res. **31** (2008), 591–656.
[6] J. Erdmann. *Combining adaptive junction control with simultaneous green-light-optimal-speed-advisory*, Proceedings of the IEEE 5th International Symposium on Wireless Vehicular Communications (WiVeC), Dresden, 2013.
[7] Forschungsgesellschaft für Straßen- und Verkehrswesen e.V, *Handbuch für die Bemessung von Straßenverkehrsanlagen*, FGSV-Verlag, Köln, 2001.
[8] J. Frasch, Parallel algorithms for optimization of dynamic systems in real-time, Ph.D. thesis, Otto-von-Guericke University Magdeburg, Germany, 2014.
[9] D. Frick, A. Domahidi, and M. Morari, *Embedded optimization for mixed logical dynamical systems*, Comput. Chem. Eng. **72** (2015), 21–33.
[10] B. Friedrich, P. Wagner, W. Niebel, A. Herrmann, S. Naumann, O. Bley, O. Kutzner, M. Maurer, F. Saust, T. Schüler, H. Poppe, M. Junge, and J. Langenberg. *KOLINE: Kooperative und optimierte Lichtsignalsteuerung in städtischen Netzen: Schlussbericht zum Forschungsprojekt, Förderkennzeichen 19P9002, gefördert vom Bundesministerium für Wirtschaft und Technologie*. 2013.
[11] R. Gallager, *Stochastic processes: Theory for applications*, Cambridge University Press, Cambridge, MA, 2013.
[12] A. Giridhar and P. Kumar, *Scheduling automated traffic on a network of roads*, IEEE Trans. Veh. Technol. **55** (2006), no. 5, 1467–1474. https://doi.org/10.1109/TVT.2006.877472
[13] Q. Guo, L. Li, and X. J. Ban, *Urban traffic signal control with connected and automated vehicles: A survey*, Transp. Res. C Emerg. Technol **101** (2019), 313–334. https://doi.org/10.1016/j.trc.2019.01.026. Available from, http://www.sciencedirect.com/science/article/pii/S0968090X18311641

[14] R. Hult, G. R. Campos, P. Falcone, and H. Wymeersch, *An approximate solution to the optimal coordination problem for autonomous vehicles at intersections*, Proceedings of the 2015 American Control Conference (ACC), Chicago, 2015, pp. 763–768.
[15] R. Hult, M. Zanon, S. Gros, and P. Falcone, *An MIQP-based heuristic for optimal coordination of vehicles at intersections*, Proceedings of the 2018 IEEE Conference on Decision and Control (CDC), Miami, 2018, pp. 2783–2790.
[16] R. Hult, M. Zanon, S. Gros, and P. Falcone, *Optimal coordination of automated vehicles at intersections: Theory and experiments*, IEEE Trans. Control Syst. Technol. **27** (2018), no. 6, 2510–2525.
[17] A. Kesting, M. Treiber, and D. Helbing, *Enhanced intelligent driver model to access the impact of driving strategies on traffic capacity*, Philos. Trans. Royal Soc. A Math. Phys. Eng. Sci. **368** (2010), no. 1928, 4585–4605. https://doi.org/10.1098/rsta.2010.0084
[18] M. Khayatian, M. Mehrabian, E. Andert, R. Dedinsky, S. Choudhary, Y. Lou, and A. Shirvastava, *A survey on intersection management of connected autonomous vehicles*, ACM Trans. Cyber-Phys. Syst. **4** (2020), no. 4, 1–27.
[19] D. Krajzewicz, J. Erdmann, M. Behrisch, and L. Bieker, *Recent development and applications of SUMO-simulation of urban mobility*, Int. J. Adv. Syst. Measur **5** (2012), nos. 3 and 4, 128–138.
[20] S. Krauß, Microscopic modeling of traffic flow: Investigation of collision free vehicle dynamics, Ph.D. thesis, 1998.
[21] S. Le Vine, A. Zolfaghari, and J. Polak, *Autonomous cars: The tension between occupant experience and intersection capacity*, Transp Res C Emerg Technol **52** (2015), 1–14.
[22] J. Lee and B. Park, *Development and evaluation of a cooperative vehicle intersection control algorithm under the connected vehicles environment*, IEEE Trans Intell Transp Syst **13** (2012), no. 1, 81–90. https://doi.org/10.1109/TITS.2011.2178836
[23] J. Lee, J. Leung, and F. Margot, *Min-up/min-down polytopes*, Discr Optim **1** (2004), no. 1, 77–85.
[24] L. Li, D. Wen, and D. Yao, *A survey of traffic control with vehicular communications*, IEEE Trans. Intell. Transp. Syst. **15** (2014), no. 1, 425–432. https://doi.org/10.1109/TITS.2013.2277737
[25] Z. Li, L. Elefteriadou, and S. Ranka, *Signal control optimization for automated vehicles at isolated signalized intersections*, Transp. Res. C Emerg. Technol. **49** (2014), 1–18.
[26] A. A. Malikopoulos, C. G. Cassandras, and Y. J. Zhang, *A decentralized energy-optimal control framework for connected automated vehicles at signal-free intersections*, Automatica **93** (2018), 244–256.
[27] K. Oeltze and E. Stemmler. Interdisziplinäre Bewertung der Auswirkung eines Fahrers mit Ampelassistenz auf nicht-ausgestattete Fahrer, Proceedings of the 8. VDI-Tagung: Fahrer im 21. Jahrhundert, Braunschweig, 2015.
[28] R. Oertel and P. Wagner, *Delay-time actuated traffic signal control for an isolated intersection*, Proceedings of the 90th Annual Meeting Transportation Research Board (TRB), Washington, D.C., 2011.
[29] R. Oertel, J. Erdmann, T. Hesse, R. Markowski, J. Trumpold, and P. Wagner. Vital: Traffic signal control based on C2I communication data-application and results from the field, Proceedings of the mobil.TUM 2017 - Intelligent Transport Systems in Theory and Practice, München, 2017.
[30] D. Rajan and S. Takriti, *Minimum up/down polytopes of the unit commitment problem with start-up costs*, IBM Res. Rep. **23628** (2005), 1–14.
[31] J. B. Rawlings, D. Q. Mayne, and M. Diehl, *Model predictive control: Theory, computation, and design*, Vol **2**, Nob Hill Publishing, Madison, WI, 2017.
[32] J. Rios-Torres and A. A. Malikopoulos, *A survey on the coordination of connected and automated vehicles at intersections and merging at highway on-ramps*, IEEE Trans. Intell. Transp. Syst. **18** (2017), no. 5, 1066–1077. https://doi.org/10.1109/TITS.2016.2600504
[33] C. Schießl and K. Oeltze, *Benefits and challenges of multi-driver simulator studies*, IET Intell. Transp. Syst. **9** (2015), no. 6, 618–625. https://doi.org/10.1049/iet-its.2014.0210
[34] L. Schnieder and R. Krenkel, Betreibermodell einer Forschungsinfrastruktur für die Entwicklung intelligenter Mobilitätsdienste im realen Verkehrsumfeld, Proceedings of the Symposium Automatisierungssysteme, Assistenzsysteme und eingebettete Systeme für Transportmittel (AAET), Braunschweig, Vol. 16, 2015, pp. 108–116.
[35] S. Sorgatz, Optimization of vehicular traffic at traffic-light controlled intersections. Ph.D. thesis, Otto-von-Guericke University Magdeburg, 2016. https://mathopt.de/PUBLICATIONS/Sorgatz2016.pdf
[36] S. Sorgatz, F. Kranke, and H. Poppe, *Der Kreuzungslotse von Volkswagen: Urbane Assistenz für einen verbesserten Verkehrsfluss und Fahrkomfort*, Straßenverkehrstechnik **60** (2016), no. 7, 425–432.
[37] S. Takriti, B. Krasenbrink, and L. S.-Y. Wu, *Incorporating fuel constraints and electricity spot prices into the stochastic unit commitment problem*, Oper. Res. **48** (2000), no. 2, 268–280.
[38] M. Treiber, A. Hennecke, and D. Helbing, *Congested traffic states in empirical observations and microscopic simulations*, Phys. Rev. E **62** (2000), no. 2, 1805–1824. https://doi.org/10.1103/PhysRevE.62.1805
[39] Umweltbundesamt, *Handbuch emissionsfaktoren des Straßenverkehrs version 3.1*, INFRAS, Zürich, 2010.
[40] Verband der Automobilindustrie e.V *simTD - Sichere Intelligente Mobilität Testfeld Deutschland*, 2014. Available from: http://www.simtd.de/index.dhtml/deDE/index.html
[41] K. Yang, S. I. Guler, and M. Menendez, *Isolated intersection control for various levels of vehicle technology: Conventional, connected, and automated vehicles*, Transp. Res. C Emerg. Technol. **72** (2016), 109–129. https://doi.org/10.1016/j.trc.2016.08.009. Available from, http://www.sciencedirect.com/science/article/pii/S0968090X16301437
[42] Y. J. Zhang, A. A. Malikopoulos, and C. G. Cassandras, Optimal control and coordination of connected and automated vehicles at urban traffic intersections, Proceedings of the 2016 American Control Conference, Boston, 2016, pp. 6227–6232.

How to cite this article: D. D. Le, M. Merkert, S. Sorgatz, M. Hahn, and S. Sager, *Autonomous traffic at intersections: An optimization-based analysis of possible time, energy, and CO_2 savings*, Networks. **79** (2022), 338–363. https://doi.org/10.1002/net.22078

APPENDIX A: PROBLEM INSTANCES

Here, we give a list of all used problem instances and the results of the computation. Table A1 shows the separate problem instances for the global-MILP, instances from the moving-horizon approach are listed in Tables A2 and A3.

TABLE A1 Computational results on global-MILP

Name	#Cars	*T* (s)	*dt* (s)	*L* (s)	Comp. time (s)	Obj. (m)	Waiting time (s)	Arrival time (s)	Fuel (l/100 km)	CO_2 (g/km)
veryhigh-1-rw	75	60	0.5	10	—	—	13.75	54.30	10.60	246.65
veryhigh-2-rw	89	60	0.5	10	—	—	15.16	59.81	10.84	252.14
veryhigh-3-rw	91	60	0.5	10	—	—	15.94	62.97	10.95	254.65
veryhigh-4-rw	83	60	0.5	10	—	—	14.37	56.62	10.49	244.04
veryhigh-5-rw	82	60	0.5	10	—	—	14.21	56.16	10.50	244.17
veryhigh-1-fi	75	60	0.5	10	9.47	25388.9	8.03	38.99	9.12	212.23
veryhigh-2-fi	89	60	0.5	10	23.94	29382.4	8.61	39.96	9.37	217.87
veryhigh-3-fi	91	60	0.5	10	14.72	30592.9	8.22	39.15	9.26	215.41
veryhigh-4-fi	83	60	0.5	10	11.85	27969.1	8.12	39.37	9.18	213.66
veryhigh-5-fi	82	60	0.5	10	12.48	27984.8	7.76	38.54	9.02	209.92
veryhigh-1-mi	75	60	0.5	10	23445.4	26360.7	7.18	37.39	8.85	205.98
veryhigh-2-mi	89	60	0.5	10	36026.8*	31095.3*(8.27%)	7.34	37.81	8.96	208.37
veryhigh-3-mi	91	60	0.5	10	36033.8*	31569.4*(11.76%)	7.52	38.02	9.04	210.33
veryhigh-4-mi	83	60	0.5	10	36026.2*	28779.6*(6.02%)	7.48	38.10	8.95	208.23
veryhigh-5-mi	82	60	0.5	10	33190.4	28373.5	7.45	37.97	9.00	209.48
veryhigh-1-fr	75	60	0.5	—	6.88	34425.8	0.15	26.85	6.37	148.09
veryhigh-2-fr	89	60	0.5	—	12.65	40910.8	0.14	26.83	6.42	149.28
veryhigh-3-fr	91	60	0.5	—	18.87	41880.9	0.11	26.80	6.57	152.93
veryhigh-4-fr	83	60	0.5	—	11.37	38145.3	0.10	26.78	6.52	151.69
veryhigh-5-fr	82	60	0.5	—	44.75	37440.7	0.23	26.95	6.20	144.33
high-1-rw	64	60	0.5	10	—	—	12.99	51.31	10.51	244.48
high-2-rw	49	60	0.5	10	—	—	11.45	46.71	10.54	245.16
high-3-rw	59	60	0.5	10	—	—	12.41	49.61	10.54	245.28
high-4-rw	68	60	0.5	10	—	—	13.57	53.35	10.59	246.35
high-5-rw	63	60	0.5	10	—	—	12.57	50.24	10.60	246.67
high-1-fi	64	60	0.5	10	4.8	22390.2	7.31	37.60	8.70	202.31
high-2-fi	49	60	0.5	10	3.08	16885.9	7.62	38.25	8.59	199.87
high-3-fi	59	60	0.5	10	4.41	19797	8.15	39.15	8.89	206.91
high-4-fi	68	60	0.5	10	5.87	23289.8	7.73	38.25	8.89	206.93
high-5-fi	63	60	0.5	10	5.22	21170.5	8.12	39.65	9.00	209.40
high-1-mi	64	60	0.5	10	28261.6	22612.4	7.09	37.35	8.67	201.64
high-2-mi	49	60	0.5	10	15361.5	17532.7	6.75	36.69	8.46	196.87
high-3-mi	59	60	0.5	10	14243.6	20990.8	6.83	36.87	8.50	197.76
high-4-mi	68	60	0.5	10	29758.2	24380.2	6.68	36.58	8.69	202.05
high-5-mi	63	60	0.5	10	13725.2	22390.8	6.84	36.94	8.72	202.81
high-1-fr	64	60	0.5	—	22.66	29262.4	0.30	27.04	6.26	145.73
high-2-fr	49	60	0.5	—	4.34	22496.8	0.14	26.83	6.53	151.86
high-3-fr	59	60	0.5	—	5.34	27021.1	0.15	26.85	6.42	149.28
high-4-fr	68	60	0.5	—	15.58	31284.8	0.05	26.71	6.76	157.20
high-5-fr	63	60	0.5	—	8.34	28924.5	0.08	26.75	6.59	153.29
medium-1-rw	40	60	0.5	10	—	—	11.27	46.33	10.49	243.94
medium-2-rw	36	60	0.5	10	—	—	10.00	43.03	10.39	241.79
medium-3-rw	44	60	0.5	10	—	—	11.46	46.98	10.58	246.13
medium-4-rw	31	60	0.5	10	—	—	8.87	40.78	9.85	229.15
medium-5-rw	40	60	0.5	10	—	—	10.42	44.37	10.51	244.59

(Continues)

TABLE A1 Continued

Name	#Cars	*T* (s)	*dt* (s)	*L* (s)	Comp. time (s)	Obj. (m)	Waiting time (s)	Arrival time (s)	Fuel (l/100 km)	CO_2 (g/km)
medium-1-fi	40	60	0.5	10	2.43	13448.7	8.03	38.89	8.62	200.43
medium-2-fi	36	60	0.5	10	2.11	12383	7.59	38.18	8.49	197.46
medium-3-fi	44	60	0.5	10	2.91	14605	8.40	39.81	8.95	208.19
medium-4-fi	31	60	0.5	10	1.78	10874.8	7.19	37.77	8.21	191.01
medium-5-fi	40	60	0.5	10	2.16	13463.2	8.01	39.14	8.71	202.52
medium-1-mi	40	60	0.5	10	1279.52	14880.8	5.68	34.99	8.13	189.11
medium-2-mi	36	60	0.5	10	2142.09	13239.1	6.02	35.34	8.33	193.67
medium-3-mi	44	60	0.5	10	3764.31	16405.7	5.72	35.00	8.06	187.56
medium-4-mi	31	60	0.5	10	242.81	11513.9	5.83	35.12	7.98	185.55
medium-5-mi	40	60	0.5	10	723.5	14747.6	5.90	35.16	8.21	191.08
medium-1-fr	40	60	0.5	—	1.87	18288.4	0.13	26.83	6.45	150.10
medium-2-fr	36	60	0.5	—	3.36	16497.3	0.13	26.82	6.55	152.34
medium-3-fr	44	60	0.5	—	1.55	20251.5	0.02	26.68	6.83	158.82
medium-4-fr	31	60	0.5	—	1.11	14253.4	0.08	26.76	6.56	152.54
medium-5-fr	40	60	0.5	—	3.7	18276.1	0.15	26.85	6.36	147.89
small-1-rw	23	60	0.5	10	—	—	7.89	38.92	9.54	222.00
small-2-rw	14	60	0.5	10	—	—	9.37	40.34	10.35	240.79
small-3-rw	21	60	0.5	10	—	—	8.82	40.63	10.20	237.31
small-4-rw	23	60	0.5	10	-	-	9.52	41.57	10.38	241.43
small-5-rw	23	60	0.5	10	—	—	9.68	41.68	10.71	249.07
small-1-fi	23	60	0.5	10	1.02	8433.85	6.05	35.50	8.04	187.08
small-2-fi	14	60	0.5	10	0.56	4803.89	7.49	37.22	7.96	185.14
small-3-fi	21	60	0.5	10	0.93	7286.1	7.24	37.70	8.04	187.06
small-4-fi	23	60	0.5	10	1.18	8340.56	6.28	35.98	7.91	184.02
small-5-fi	23	60	0.5	10	0.9	8025.56	7.33	37.30	8.22	191.33
small-1-mi	23	60	0.5	10	86.76	8803.14	4.99	33.80	7.82	182.00
small-2-mi	14	60	0.5	10	13.57	5630.63	3.62	31.62	7.48	174.10
small-3-mi	21	60	0.5	10	643.75	7777.55	5.69	34.92	7.67	178.36
small-4-mi	23	60	0.5	10	197.18	8603.8	5.52	34.55	7.87	183.12
small-5-mi	23	60	0.5	10	113.74	9233.69	3.89	32.03	7.73	179.78
small-1-fr	23	60	0.5	—	0.81	10536.1	0.09	26.77	6.59	153.24
small-2-fr	14	60	0.5	—	0.46	6407.25	0.03	26.69	6.84	159.20
small-3-fr	21	60	0.5	—	1.09	9540.4	0.25	26.98	6.37	148.12
small-4-fr	23	60	0.5	—	1.05	10520.8	0.11	26.79	6.60	153.62
small-5-fr	23	60	0.5	—	2.47	10564.2	0.14	26.83	6.54	152.09
geom. mean veryhigh-rw	83.8063	60	0.5	10	—	—	14.6659	57.8923	10.6744	248.293
geom. mean veryhigh-fi	83.8063	60	0.5	10	13.7614	28209.2	8.14332	39.1992	9.18923	213.801
geom. mean veryhigh-mi	83.8063	60	0.5	10	32524.1	29173.1	7.39298	37.8572	8.95977	208.473
geom. mean veryhigh-fr	83.8063	60	0.5	—	15.2898	38468.4	0.139659	26.8419	6.41469	149.234
geom. mean high-rw	60.2304	60	0.5	10	—	—	12.5783	50.1965	10.5559	245.587
geom. mean high-fi	60.2304	60	0.5	10	4.57202	20578.6	7.77953	38.5732	8.81275	205.055
geom. mean high-mi	60.2304	60	0.5	10	19075.5	21451.9	6.83661	36.8851	8.60734	200.211
geom. mean high-fr	60.2304	60	0.5	—	9.26414	27627.8	0.120304	26.8358	6.50985	151.423
geom. mean medium-rw	37.9356	60	0.5	10	—	—	10.3605	44.2402	10.3606	241.04
geom. mean medium-fi	37.9356	60	0.5	10	2.24766	12891.9	7.83285	38.7513	8.59251	199.841
geom. mean medium-mi	37.9356	60	0.5	10	1126.3	14056.7	5.82871	35.1218	8.1411	189.373
geom. mean medium-fr	37.9356	60	0.5	—	2.09126	17392.8	0.0834871	26.7879	6.54812	152.295
geom. mean small-rw	20.4506	60	0.5	10	—	—	9.03149	40.6156	10.2286	237.949
geom. mean small-fi	20.4506	60	0.5	10	0.891824	7230.31	6.85185	36.7302	8.03331	186.909
geom. mean small-mi	20.4506	60	0.5	10	111.193	7892.61	4.66404	33.3574	7.71279	179.444
geom. mean small-fr	20.4506	60	0.5	—	1.01044	9353.21	0.100778	26.8118	6.58629	153.213

TABLE A2 Computational results for the moving horizon approach with a sampling period of five time steps (i.e., 2.5 s) and varying lengths of the prediction horizon for instances with medium and very high traffic density

Name	#Cars	T (s)	dt	L	Comp. time MILP (s)	Max MILP (s)	Obj. MILP (m)	Waiting time (s)	Arrival time (s)	Fuel (l/100 km)	CO_2 (g/km)
veryhigh-1-mi-10-5	75	60	0.5	10	9.45	1.41	23164.4	9.91	43.06	11.20	260.63
veryhigh-1-mi-15-5	75	60	0.5	10	24.94	3.72	23130.9	9.97	43.42	11.57	269.12
veryhigh-1-mi-20-5	75	60	0.5	10	73.88	10.93	24159.9	9.10	41.23	10.56	245.69
veryhigh-1-mi-25-5	75	60	0.5	10	135.44	17.36	24300.5	8.97	41.02	9.77	227.27
veryhigh-1-mi-30-5	75	60	0.5	10	231.70	28.17	25077.8	8.29	39.70	9.14	212.62
veryhigh-1-mi-35-5	75	60	0.5	10	314.95	55.81	25207.6	8.19	39.59	9.23	214.65
veryhigh-1-mi-40-5	75	60	0.5	10	408.65	42.84	25531.0	7.90	39.07	9.26	215.39
veryhigh-1-mi-45-5	75	60	0.5	10	564.16	59.85	25081.5	8.29	39.78	9.11	212.00
veryhigh-1-mi-50-5	75	60	0.5	10	669.87	63.33	25884.2	7.59	38.38	9.02	209.75
veryhigh-1-mi-55-5	75	60	0.5	10	759.87	67.77	25927.0	7.56	38.31	9.25	215.12
veryhigh-1-mi-60-5	75	60	0.5	10	1071.93	151.50	25922.9	7.56	38.32	9.31	216.64
veryhigh-1-fi	75	60	0.5	10	9.47	—	25388.9	8.03	38.99	9.12	212.23
veryhigh-1-mi	75	60	0.5	10	23445.40	—	26360.7	7.18	37.39	8.85	205.98
veryhigh-2-mi-10-5	89	60	0.5	10	9.49	1.18	28176.5	9.43	42.11	10.78	250.81
veryhigh-2-mi-15-5	89	60	0.5	10	42.59	6.67	28543.4	9.20	41.59	10.11	235.17
veryhigh-2-mi-20-5	89	60	0.5	10	115.71	14.54	29216.0	8.73	40.64	10.11	235.27
veryhigh-2-mi-25-5	89	60	0.5	10	215.64	28.26	29667.0	8.40	40.20	8.77	204.01
veryhigh-2-mi-30-5	89	60	0.5	10	300.24	27.64	30286.3	7.94	38.92	9.18	213.63
veryhigh-2-mi-35-5	89	60	0.5	10	492.79	57.12	30589.8	7.71	38.58	9.02	209.81
veryhigh-2-mi-40-5	89	60	0.5	10	625.90	61.47	30690.3	7.64	38.44	9.13	212.37
veryhigh-2-mi-45-5	89	60	0.5	10	733.61	87.72	30187.3	8.02	39.22	9.45	219.92
veryhigh-2-mi-50-5	89	60	0.5	10	1013.91	98.72	30444.9	7.83	38.85	9.50	221.07
veryhigh-2-mi-55-5	89	60	0.5	10	1371.88	144.80	30502.1	7.78	38.71	9.24	215.00
veryhigh-2-mi-60-5	89	60	0.5	10	1600.14	189.69	30586.5	7.72	38.68	9.16	212.98
veryhigh-2-fi	89	60	0.5	10	23.94	—	29382.4	8.61	39.96	9.37	217.87
veryhigh-2-mi	89	60	0.5	10	36026.8*	—	31095.3*(8.27%)	7.34	37.81	8.96	208.37
veryhigh-3-mi-10-5	91	60	0.5	10	12.62	1.42	28526.5	9.67	42.30	11.77	273.72
veryhigh-3-mi-15-5	91	60	0.5	10	52.30	8.15	29063.7	9.29	41.71	10.67	248.33
veryhigh-3-mi-20-5	91	60	0.5	10	98.40	15.61	30041.6	8.62	40.41	10.80	251.18
veryhigh-3-mi-25-5	91	60	0.5	10	187.33	22.56	29987.2	8.69	40.83	10.01	232.76
veryhigh-3-mi-30-5	91	60	0.5	10	338.73	40.44	30090.2	8.59	40.49	9.96	231.70
veryhigh-3-mi-35-5	91	60	0.5	10	435.88	44.55	31011.7	7.93	39.02	9.08	211.23
veryhigh-3-mi-40-5	91	60	0.5	10	638.31	61.57	31311.1	7.71	38.58	9.69	225.34
veryhigh-3-mi-45-5	91	60	0.5	10	835.11	89.08	31279.3	7.73	38.62	9.74	226.55
veryhigh-3-mi-50-5	91	60	0.5	10	1022.37	128.65	31290.1	7.72	38.61	9.62	223.68
veryhigh-3-mi-55-5	91	60	0.5	10	1317.32	136.22	31188.3	7.80	38.85	9.54	222.02
veryhigh-3-mi-60-5	91	60	0.5	10	1764.90	170.54	31368.4	7.66	38.54	9.46	220.10
veryhigh-3-fi	91	60	0.5	10	14.72	—	30592.9	8.22	39.15	9.26	215.41
veryhigh-3-mi	91	60	0.5	10	36033.8*	—	31569.4*(11.76%)	7.52	38.02	9.04	210.33
veryhigh-4-mi-10-5	83	60	0.5	10	7.70	1.01	25481.6	10.03	43.31	12.41	288.60
veryhigh-4-mi-15-5	83	60	0.5	10	42.01	6.91	26755.9	9.07	41.08	10.80	251.35
veryhigh-4-mi-20-5	83	60	0.5	10	80.80	11.09	26953.7	8.91	40.96	10.90	253.55
veryhigh-4-mi-25-5	83	60	0.5	10	180.15	20.94	27150.4	8.76	40.69	10.03	233.36
veryhigh-4-mi-30-5	83	60	0.5	10	266.32	25.12	27943.1	8.13	39.54	9.53	221.79
veryhigh-4-mi-35-5	83	60	0.5	10	452.25	46.81	28165.2	7.96	39.06	9.48	220.52
veryhigh-4-mi-40-5	83	60	0.5	10	487.94	48.38	28150.8	7.97	39.19	9.67	224.93
veryhigh-4-mi-45-5	83	60	0.5	10	623.53	62.20	27920.7	8.16	39.53	9.88	229.73

(Continues)

TABLE A2 Continued

Name	#Cars	T (s)	dt	L	Comp. time MILP (s)	Max MILP (s)	Obj. MILP (m)	Waiting time (s)	Arrival time (s)	Fuel (l/100 km)	CO_2 (g/km)
veryhigh-4-mi-50-5	83	60	0.5	10	801.90	90.91	28185.6	7.95	39.12	9.72	226.04
veryhigh-4-mi-55-5	83	60	0.5	10	1156.58	136.90	28133.6	7.99	39.22	9.56	222.43
veryhigh-4-mi-60-5	83	60	0.5	10	1531.53	149.78	28177.1	7.95	39.13	9.59	223.08
veryhigh-4-fi	83	60	0.5	10	11.85	—	27969.1	8.12	39.37	9.18	213.66
veryhigh-4-mi	83	60	0.5	10	36026.2*	—	28779.6*(6.02%)	7.48	38.10	8.95	208.23
veryhigh-5-mi-10-5	82	60	0.5	10	10.42	1.60	26294.2	9.06	41.26	11.06	257.27
veryhigh-5-mi-15-5	82	60	0.5	10	38.42	7.03	26347.5	9.06	41.14	10.61	246.78
veryhigh-5-mi-20-5	82	60	0.5	10	76.74	14.19	26756.8	8.74	40.61	10.48	243.77
veryhigh-5-mi-25-5	82	60	0.5	10	164.26	22.24	26762.3	8.73	40.59	9.86	229.28
veryhigh-5-mi-30-5	82	60	0.5	10	308.76	35.70	27460.0	8.18	39.44	9.50	221.03
veryhigh-5-mi-35-5	82	60	0.5	10	387.15	40.45	27572.7	8.09	39.32	9.33	216.94
veryhigh-5-mi-40-5	82	60	0.5	10	524.48	49.21	27588.5	8.08	39.49	9.58	222.94
veryhigh-5-mi-45-5	82	60	0.5	10	704.97	69.48	27958.2	7.78	38.74	9.44	219.59
veryhigh-5-mi-50-5	82	60	0.5	10	818.30	81.98	27782.7	7.93	39.12	9.47	220.30
veryhigh-5-mi-55-5	82	60	0.5	10	1243.88	118.24	27858.1	7.87	39.01	9.55	222.10
veryhigh-5-mi-60-5	82	60	0.5	10	1598.36	194.72	27859.7	7.86	39.01	9.53	221.65
veryhigh-5-fi	82	60	0.5	10	12.48	—	27984.8	7.76	38.54	9.02	209.92
veryhigh-5-mi	82	60	0.5	10	33190.40	—	28373.5	7.45	37.97	9.00	209.48
medium-1-mi-10-5	40	60	0.5	10	6.60	0.89	13953.9	7.16	37.42	10.41	242.07
medium-1-mi-15-5	40	60	0.5	10	13.24	1.84	13437.7	8.02	39.03	9.57	222.68
medium-1-mi-20-5	40	60	0.5	10	17.75	2.02	14025.0	7.08	37.11	9.33	217.08
medium-1-mi-25-5	40	60	0.5	10	40.60	4.62	14599.8	6.14	35.73	8.47	197.15
medium-1-mi-30-5	40	60	0.5	10	69.15	13.55	14853.1	5.73	35.06	8.04	186.98
medium-1-mi-35-5	40	60	0.5	10	92.81	10.44	14873.1	5.70	35.01	8.11	188.63
medium-1-mi-40-5	40	60	0.5	10	128.48	16.47	14861.2	5.72	35.04	8.10	188.34
medium-1-mi-45-5	40	60	0.5	10	159.26	15.61	14873.2	5.70	35.01	8.13	189.04
medium-1-mi-50-5	40	60	0.5	10	230.13	33.35	14759.5	5.88	35.25	8.21	190.91
medium-1-mi-55-5	40	60	0.5	10	273.36	24.37	14759.1	5.90	35.30	7.80	181.45
medium-1-mi-60-5	40	60	0.5	10	290.58	28.43	14759.5	5.88	35.25	8.29	192.74
medium-1-fi	40	60	0.5	10	2.43	—	13448.7	8.03	38.89	8.62	200.43
medium-1-mi	40	60	0.5	10	1279.52	—	14880.8	5.68	34.99	8.13	189.11
medium-2-mi-10-5	36	60	0.5	10	5.88	0.91	11617.8	8.93	40.69	10.58	246.15
medium-2-mi-15-5	36	60	0.5	10	18.16	2.21	11087.6	9.93	42.95	11.01	256.05
medium-2-mi-20-5	36	60	0.5	10	22.79	3.29	11977.4	8.32	39.50	8.73	203.17
medium-2-mi-25-5	36	60	0.5	10	38.41	4.78	12781.0	6.86	36.99	8.40	195.41
medium-2-mi-30-5	36	60	0.5	10	64.68	7.90	12782.1	6.89	36.96	7.75	180.32
medium-2-mi-35-5	36	60	0.5	10	98.55	10.12	12771.5	6.88	36.88	8.31	193.35
medium-2-mi-40-5	36	60	0.5	10	128.50	11.39	12951.8	6.55	36.40	8.06	187.55
medium-2-mi-45-5	36	60	0.5	10	163.13	13.93	12866.0	6.71	36.66	8.37	194.69
medium-2-mi-50-5	36	60	0.5	10	203.08	18.65	12905.5	6.64	36.53	8.38	195.01
medium-2-mi-55-5	36	60	0.5	10	219.25	19.78	12985.4	6.49	36.24	8.45	196.58
medium-2-mi-60-5	36	60	0.5	10	270.11	24.80	12978.1	6.51	36.30	8.64	200.96
medium-2-fi	36	60	0.5	10	2.11	—	12383.0	7.59	38.18	8.49	197.46

(Continues)

TABLE A2 Continued

Name	#Cars	T (s)	dt	L	Comp. time MILP (s)	Max MILP (s)	Obj. MILP (m)	Waiting time (s)	Arrival time (s)	Fuel (l/100 km)	CO_2 (g/km)
medium-2-mi	36	60	0.5	10	2142.09	—	13239.1	6.02	35.34	8.33	193.67
medium-3-mi-10-5	44	60	0.5	10	5.62	0.82	15068.7	7.66	38.28	10.48	243.71
medium-3-mi-15-5	44	60	0.5	10	11.55	1.43	15238.6	7.44	37.91	10.24	238.27
medium-3-mi-20-5	44	60	0.5	10	23.98	4.17	15325.5	7.31	37.74	9.38	218.23
medium-3-mi-25-5	44	60	0.5	10	56.72	6.48	15679.0	6.80	36.79	8.71	202.62
medium-3-mi-30-5	44	60	0.5	10	91.79	9.81	16125.4	6.13	35.62	8.13	189.11
medium-3-mi-35-5	44	60	0.5	10	117.88	10.40	16179.8	6.05	35.48	8.26	192.23
medium-3-mi-40-5	44	60	0.5	10	165.72	15.60	16396.6	5.73	35.02	8.06	187.54
medium-3-mi-45-5	44	60	0.5	10	200.70	23.07	16396.6	5.73	35.02	8.02	186.48
medium-3-mi-50-5	44	60	0.5	10	254.61	26.65	16290.9	5.89	35.21	8.19	190.51
medium-3-mi-55-5	44	60	0.5	10	283.24	22.77	16396.0	5.74	35.04	7.57	176.17
medium-3-mi-60-5	44	60	0.5	10	380.64	30.54	16286.0	5.89	35.24	8.26	192.09
medium-3-fi	44	60	0.5	10	2.91	—	14605.0	8.40	39.81	8.95	208.19
medium-3-mi	44	60	0.5	10	3764.31	—	16405.7	5.72	35.00	8.06	187.56
medium-4-mi-10-5	31	60	0.5	10	5.46	0.69	9534.5	9.92	43.56	10.98	255.39
medium-4-mi-15-5	31	60	0.5	10	9.38	1.82	10295.4	8.40	39.82	10.40	241.89
medium-4-mi-20-5	31	60	0.5	10	14.27	2.24	10487.3	8.00	39.14	9.59	223.21
medium-4-mi-25-5	31	60	0.5	10	34.79	3.43	10653.8	7.65	38.24	9.30	216.30
medium-4-mi-30-5	31	60	0.5	10	44.57	5.26	11023.4	6.88	37.09	8.28	192.62
medium-4-mi-35-5	31	60	0.5	10	72.37	7.27	11146.7	6.61	36.56	8.14	189.34
medium-4-mi-40-5	31	60	0.5	10	99.65	15.14	11191.4	6.52	36.36	8.24	191.71
medium-4-mi-45-5	31	60	0.5	10	117.18	11.85	11329.5	6.24	35.94	8.13	189.05
medium-4-mi-50-5	31	60	0.5	10	133.11	19.12	11345.8	6.22	35.91	7.84	182.27
medium-4-mi-55-5	31	60	0.5	10	171.34	18.08	11352.0	6.19	35.84	7.94	184.80
medium-4-mi-60-5	31	60	0.5	10	221.85	23.96	11364.8	6.16	35.79	8.01	186.24
medium-4-fi	31	60	0.5	10	1.78	—	10874.8	7.19	37.77	8.21	191.01
medium-4-mi	31	60	0.5	10	242.81	—	11513.9	5.83	35.12	7.98	185.55
medium-5-mi-10-5	40	60	0.5	10	6.45	0.72	13460.0	7.98	38.73	10.38	241.50
medium-5-mi-15-5	40	60	0.5	10	11.49	1.64	13606.5	7.76	38.41	10.15	236.19
medium-5-mi-20-5	40	60	0.5	10	18.73	2.30	13908.4	7.27	37.64	9.28	215.95
medium-5-mi-25-5	40	60	0.5	10	38.41	4.99	14390.0	6.49	36.27	8.40	195.39
medium-5-mi-30-5	40	60	0.5	10	68.07	8.93	14458.2	6.38	36.10	7.99	185.93
medium-5-mi-35-5	40	60	0.5	10	110.18	14.53	14480.3	6.34	36.03	8.06	187.44
medium-5-mi-40-5	40	60	0.5	10	134.68	15.03	14332.3	6.60	36.54	7.63	177.39
medium-5-mi-45-5	40	60	0.5	10	186.90	17.88	14319.9	6.60	36.53	8.15	189.54
medium-5-mi-50-5	40	60	0.5	10	206.25	19.74	14258.3	6.70	36.74	8.11	188.64
medium-5-mi-55-5	40	60	0.5	10	270.38	27.75	14436.9	6.41	36.25	8.24	191.72
medium-5-mi-60-5	40	60	0.5	10	303.01	36.25	14436.4	6.41	36.24	8.28	192.51
medium-5-fi	40	60	0.5	10	2.16	—	13463.2	8.01	39.14	8.71	202.52
medium-5-mi	40	60	0.5	10	723.50	—	14747.6	5.90	35.16	8.21	191.08

TABLE A3 Computational results on the moving-horizon approach

Name	#Cars	*T* (s)	*dt* (s)	*L* (s)	Comp. time MILP (s)	Max MILP (s)	Obj. MILP (m)	Waiting time (s)	Arrival time (s)	Fuel (l/100 km)	CO_2 (g/km)
veryhigh-1-mi	75	60	0.5	10	296.43	91.75	25560.6	7.88	38.90	8.99	209.14
veryhigh-2-mi	89	60	0.5	10	290.38	83.28	30633.8	7.68	38.52	9.01	209.57
veryhigh-3-mi	91	60	0.5	10	277.84	74.13	31261.8	7.74	38.65	9.46	220.10
veryhigh-4-mi	83	60	0.5	10	265.27	61.87	28195.4	7.93	39.02	9.43	219.39
veryhigh-5-mi	82	60	0.5	10	232.94	55.72	27489.1	8.15	39.48	9.39	218.44
high-1-mi	64	60	0.5	10	219.21	60.55	22163.9	7.54	38.27	8.75	203.45
high-2-mi	49	60	0.5	10	120.11	35.25	17191.6	7.20	37.56	8.86	206.01
high-3-mi	59	60	0.5	10	139.83	44.45	20330.3	7.56	38.36	8.54	198.63
high-4-mi	68	60	0.5	10	222.27	74.8	23624.1	7.40	38.05	8.77	204.11
high-5-mi	63	60	0.5	10	154.96	37.41	21756.7	7.51	38.34	8.78	204.28
medium-1-mi	40	60	0.5	10	79.42	17.49	14867.3	5.71	35.05	8.06	187.40
medium-2-mi	36	60	0.5	10	57.83	13.15	12941.5	6.57	36.46	8.15	189.57
medium-3-mi	44	60	0.5	10	165.11	65.95	16171.2	6.07	35.50	8.17	190.12
medium-4-mi	31	60	0.5	10	51.32	12.68	10856.2	7.21	37.63	8.12	188.96
medium-5-mi	40	60	0.5	10	71.49	18.55	14480.3	6.34	36.03	8.02	186.67
small-1-mi	23	60	0.5	10	21.34	5.23	8803.14	4.99	33.79	7.17	166.79
small-2-mi	14	60	0.5	10	9.56	3.07	5506.95	4.21	32.50	7.15	166.37
small-3-mi	21	60	0.5	10	31.58	12.33	7578.9	6.32	35.89	7.45	173.34
small-4-mi	23	60	0.5	10	33.25	8.43	8348.02	6.26	35.89	7.66	178.27
small-5-mi	23	60	0.5	10	21.51	4.8	9233.68	3.90	32.03	7.31	169.99
geom. mean veryhigh-mi	83.8063	60	0.5	10	271.60	72.13	28551.24	7.8743	38.9126	9.2536	215.272
geom. mean high-mi	60.2304	60	0.5	10	166.20	48.40	20893.49	7.4408	38.1148	8.73934	203.281
geom. mean medium-mi	37.9356	60	0.5	10	77.42	20.44	13736.71	6.36038	36.1232	8.10381	188.539
geom. mean small-mi	20.4506	60	0.5	10	21.51	6.04	7770.03	5.03672	33.9809	7.34557	170.895

Note: The prediction horizon was set to 20 s and the sampling period to 7.5 s.